UNIVERSITÀ DEGLI STUDI DI PADOVA
Department of Molecular Medicine (DMM)

UNIVERSITY OF OXFORD
Department of Physiology, Anatomy and Genetics (DPAG)

Second cycle degree in Medical Biotechnologies

Investigating the role of hippocampal neurogenesis in Alzheimer's disease.

Supervisor:
Prof.ssa Sara Richter

Co-supervisor:
Prof. Mario Bortolozzi

External supervisor:
Prof. Francis Szele

Assistant supervisor:
Jun Yi Ong

Student:
Sabina Ciaghi

Academic year 2021/2022

Index

Abstract

Neurogenesis is a form of plasticity that occurs constitutively in the neurogenic niches of the mammalian brain. Immature granule cells arising from adult hippocampal neurogenic niche, contribute to unique brain functions in rodents and recent evidences suggests that this process persists throughout life in mammals, including humans. Importantly, studies have also found that hippocampal neurogenesis is impaired in neurodegenerative diseases; most of them concentrate on Alzheimer's disease. Given the fact the aetiology of this pathology is still unknown and several developed therapies are ineffective for the majority of patients, the study of hippocampal neurogenesis in this condition can provide insights and solutions.

In this study we evaluate the neurogenic ability of OXS-N1. This small molecule was discovered as a pro-neurogenic compound through an *in vitro* phenotypic screening employing primary cell lines from the brain of postnatal mice. It was proven to increase both proliferation and neuronal differentiation of stem and progenitor cells of the two post-natal neurogenic niches. OXS-N1 was subsequently analysed *in vivo* in wild type mice and in a familial Alzheimer's disease mouse model (5xFAD). After an evaluation of its effects on memory functions, here we perform an histological analysis on the brain tissues of these mice to assess the impact of OXS-N1 in the subgranular zone. The results we obtained indicate that OXS-N1 does not have the ability to increase the birth or survival of new neurones and neuroblasts, or to induce neural stem cells exit from quiescence. Nevertheless, these data provided an insight in the limitations of OXS-N1 applications in this experimental setting and pointed out the weaknesses of the workflow for the *in vivo* assessment of the drug's effects on adult hippocampal neurogenesis.

Introduction

1. Adult neurogenesis

The phenomenon of adult neurogenesis refers to the presence of neuronal stem cells in the adult mammalian brain that proliferate and give rise to new neurons. The two locations for adult neurogenesis are the subgranular zone (SGZ) of the dentate gyrus (DG) in the hippocampus, and the subventricular (SVZ) or subependymal zone in the lateral ventricles (LVs).

Since the beginning of the XX century, the neuroscientist S. Ramòn y Cajal established with his studies the dogma stating that neurones are generated during embryonic development and postnatal neurogenesis is not possible. However, in the 1960's, Altman and Das consistently challenged for the first time this belief: they labelled the DNA of proliferative cells in rat brains with injections of tritiated thymidine, showing that neurones are able to proliferate in the adult mammalian brain. In particular, they observed labelled nuclei in the 'basal region' of the granular cell layer of the dentate gyrus (Figure 1). Indeed, the number of proliferating cells was high in rats injected at ten days of age with a decline in frequency in mice injected at older ages (Altman and Das,1965). The same was shown in the 90's by several studies conducted in rodents (Kuhn et al., 1996) and primates (Gould et al., 1999a)(Kornack and Rakic, 1999) using BrdU labelling and immunohistochemistry for markers of newborn neurones to confirm the neuronal identity of the proliferating cell. These studies confirmed again the decline in proliferating cells in SGZ associated with aging (Kuhn et al., 1996)(Gould et al., 1999a).

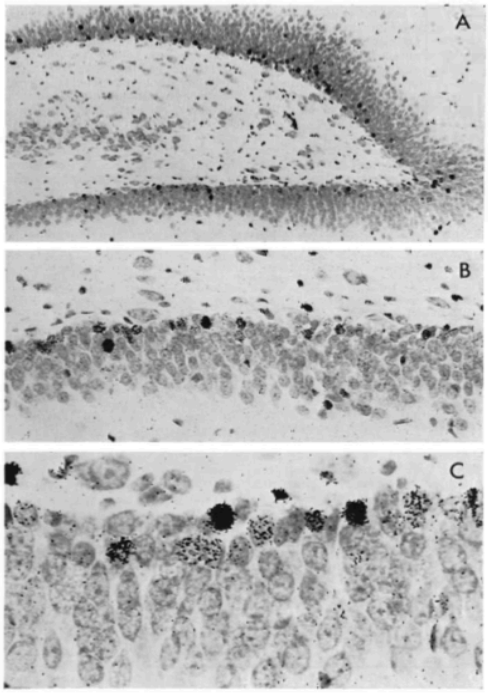

Figure 1. Image from the original paper by Altman and Das (1965). Autoradiograms of the rat dentate gyrus with proliferating cells labelled with tritriated thymidine.

In the same period, Alvarez-Buylla demonstrated the proliferation of bipotent cells, able to generate both neurones and glial cells, in the adult rodent SVZ using ^{3}H-thymidine (Lois and Alvarez-Buylla, 1993). This study was followed by another publication in which Alvarez-Buylla and Doetsch demonstrated the migration of neuronal precursors cells from the SVZ through the rostral migratory stream (RMS), to arrive at the olfactory bulb where they integrate in circuits as interneurones (Doetsch and Alvarez-Buylla, 1996). It was further demonstrated that mice deficient for these rostral migrating neurones present an impaired odor discrimination ability, providing evidence for the functional contribution of newly integrated interneurones in olfaction (Gheusi et al., 2000).

1.2. Adult hippocampal neurogenesis (AHN)

The dentate gyrus of the hippocampus harbours one of the two neurogenic niches of the adult mammals: the subgranular zone (SGZ). The SGZ is defined as a two- to three-cell-layer thick region on the hilar side of the granule cell layer. In this region there are neuronal stem cells (NSCs) and other cellular components of the niche such as astrocytes, which via their processes can translate signals from the vasculature and other cells in the germinal regions, and endothelial cells and pericytes, that surround blood vessels (Doetsch, 2003).

1.2.1. Dentate gyrus

The dentate gyrus (DG) is an integral portion of the larger functional brain system called the hippocampal formation. The DG has three layers: the molecular layer (ML), the granular cell layer (GCL) and the hilus. The first layer is relatively cell-free and is occupied by the dendrites of the dentate granule cells, and by the fibers of the major input into the hippocampus - the perforant path. The principal cell layer, the granule cell layer, is made up of densely packed granule cells and has a thickness that ranges from 4 to 8 neurons. The granule cell layer encloses a cellular region, the polymorphic cell layer or hilus, where excitatory mossy cells reside. At the boundary of the granule and hilus are located dentate pyramidal basket cells, a type of inhibitory interneuron that regulate granule cells activity.

In rodents, the dentate gyrus extends from the septal nuclei rostrally to the temporal cortex caudally, and tends to have a “V” shape septally and a “U” shape temporally. The portion of the

granule cell layer that is located between the CA3 field and the CA1 field, separated by the hippocampal fissure, is called the suprapyramidal (above CA3) blade and the portion opposite to this, the infrapyramidal (below CA3) blade. The region bridging the two blades (at the apex of the "V" or "U") is called the crest (Amaral et al., 2007) (Figure 2).

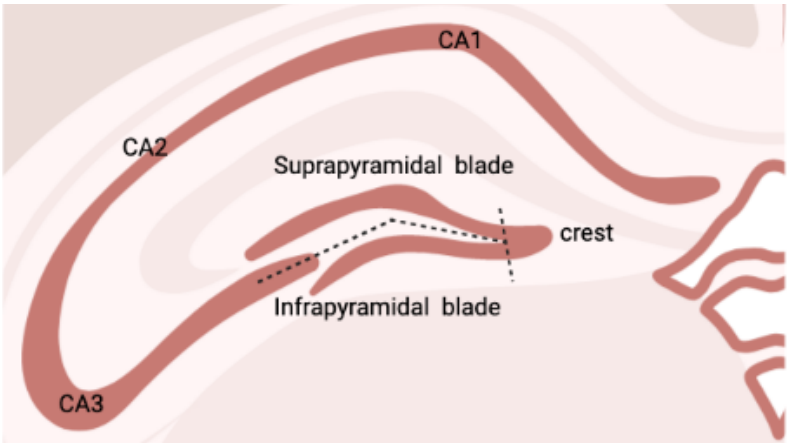

Figure 2. Murine septal dentate gyrus and its different anatomical regions.

The granule cells (GCs) of the DG have a cone-shaped tree of dendrites that extend throughout the molecular layer towards the hippocampal fissure; and the excitatory inputs to granule cells from the entorhinal cortex are on these dendritic spines. Granule cells are excitatory neurones that use glutamate as their primary transmitter. Granule cells give rise to unmyelinated axons which Ramón y Cajal called mossy fibers, that form *en passant* synapses with the mossy cells of the polymorphic layer and with the CA3 pyramidal cells of the hippocampus. Here the layer of mossy fiber termination located just above the pyramidal cell layer is called stratum lucidum (Amaral et al.,2007). The entorhinal cortex (EC) provides the major excitatory input to the dentate gyrus via axonal fibers called the perforant path. The projection to the dentate gyrus arises mainly from cells located in layer II of the entorhinal cortex, although a minor component of the projection also comes from layers V and VI. The EC receives inputs from the neocortex and limbic system. After leaving the entorhinal cortex, the fibers 'perforate' the grey matter of the subiculum and cross the hippocampal fissure to enter the dentate gyrus where they contact primarily the dendritic spines of granule cells. Then the dentate gyrus gives rise to extrinsic projections to the CA3 field of the hippocampus, and from here Schaffer's collaterals transfer stimuli to the CA1. Efferent fibers from CA1 project to the subiculum, and efferent subicular synapses project back to the EC itself (Figure 3). Since the entorhinal cortex is the source of much of the cortical sensory information that the hippocampal formation uses to carry out its functions, and since the dentate gyrus is the major

termination of projections from the entorhinal cortex, the dentate gyrus is considered to be the first step in the processing of information that ultimately leads to the production of spatial and episodic memories (Clelland et al., 2009)(Deng et al., 2010).

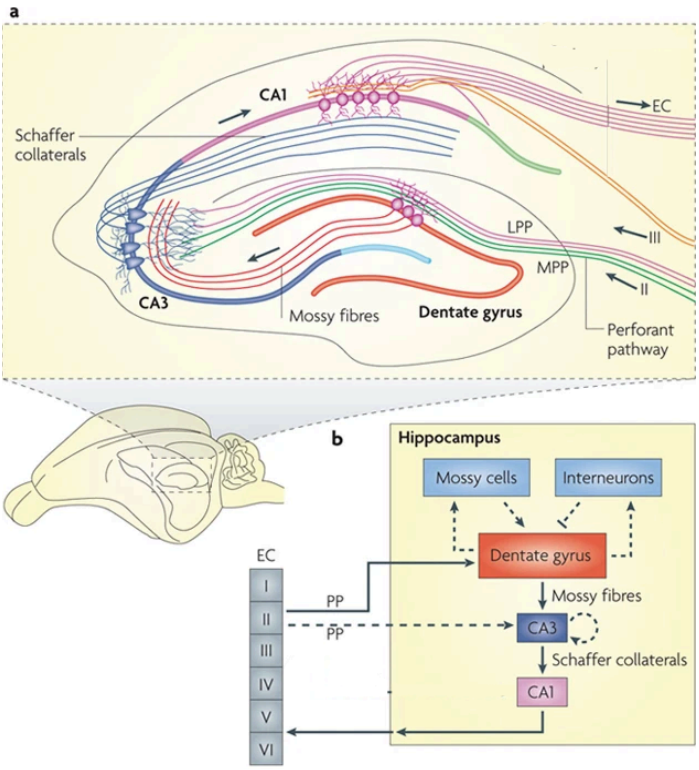

Figure 3. The perforant path and entorhinal/ hippocampal circuitry. Adapted from *Deng et al. 2010*.
(a) Major afferent and efferent connections between EC and hippocampus. (b) Diagram of the hippocampal neural network showing the traditional excitatory trisynaptic pathway: entorhinal cortex (EC)–dentate gyrus–CA3–CA1–EC.

The DG is thought to contribute to this kind of memory carrying out the function of pattern separation, which consists in the formation of distinct representations of similar inputs. This ability allows to form and use memories derived from very similar stimuli that are closely presented in space and/or time (Clelland et al., 2009). There are many reasons why the dentate gyrus is thought to have this function. First of all, at the cellular level, pattern separation is achieved through the dispersion of cortical inputs from the EC onto a greater number of dentate granule cells that are estimated to be five to ten times more in number than their principal input. Moreover, DG granule cells are finely tuned, also thanks to feedback inhibition from local interneurones, and this makes it possible that similar inputs activate distinct populations of granule cells (Deng et al., 2010).

It is worth mentioning that suprapyramidal and infrapyramidal blades have some anatomical differences. For example the length of the dendritic trees of granule cells located in the suprapyramidal blade is, on average, greater than those of cells in the infrapyramidal blade. Another difference is the spine density of these that is higher in supra- than in infapyramidal blade. Additionally, these two cell population project via mossy fibers to different regions of the CA3:

cells located in the infrapyramidal blade have axons that tend to enter CA3 in the infrapyramidal bundle, but ultimately cross the pyramidal cell layer to enter the deep portion of stratum lucidum. Cells located in the suprapyramidal blade instead enter CA3 in the stratum lucidum and continue within the most superficial portion without crossing the pyramidal layer (Chauhan et al., 2021). Another difference between the two blades is the ratio of basket cells to granule cells which is also higher in the suprapyramidal region (Amaral et al. 2007). These anatomical differences, that can reflect in circuit differences, suggest that the two blades have alternative functions; indeed several studies showed that the spatial exploration of a novel environment selectively activates the granule cells in the suprapyramidal blade (Penke et al., 2011) (Erwin et al., 2020).

1.2.2. Neural lineage progression

The process of adult neurogenesis in the hippocampus starts with quiescent neuronal stem cells (NSCs), which are also called radial glia-like (RGL) cells or type I progenitors, that when activated can divide to self-renew and/or make intermediate proliferating progenitors that eventually mature into granule cells.

Cells that *in vitro* behave as neural stem cells have been isolated from the dentate gyrus: Palmer et al. showed that adult rodent hippocampus contains multipotent progenitors and demonstrated that they can self-renew and can give rise to neurons, astrocytes, and oligodendrocytes clonal populations. This initial study was done at single-cell level by using as genetic marker a proviral integration site that is unique and identifiable for each single cells (Palmer et al., 1997). Indeed, even though the term 'neural' indicates that the differentiated fate of these cells is 'neuronal', the neural stem cells have multiple fate potentials. However, a study of Bonaguidi et al. that performed a clonal analysis of individual RGL cells over a long time period, questioned the oligodendrocytic fate of these cells under normal conditions. Additionally, this study argued that self-renewal through symmetric division represents the fate of a minority of RGLs, whereas most RGLs undergo asymmetric cell division resulting in self-renewal and differentiation into an astrocyte or neuroblast, with a frequency of the two fates that is basically equal with only a small skew towards neuronal fate (Bonaguidi et al. 2011).

In order to characterise NSCs cells *in vivo*, progenitors obtained from the adult rat hippocampus were expanded *in vitro*, labelled and implanted back into the hippocampus, where they generated new neurons and glia (Gage et al., 1995). This study was at the population level, but

was followed in more recent years by several publications using *in vivo* fate mapping (Seri et al., 2004)(Garcia et al., 2004) and lineage tracing (Suh et al., 2007) experiments that allowed researchers to demonstrate the presence of progenitors responsible for constitutive neurogenesis in the adult mouse SVZ and SGZ.

RGL cells express GFAP, nestin (Lendahl et al., 1990) and vimentin (Seri et al., 2001) as intermediate filaments, and the transcription factors Sox2 and Pax6 (Figure 3). Sox2 or SRY (sex determining region Y) box 2, expressed in embryonic stem cells and adult NSCs, is critical for stem cell proliferation and differentiation (Suh et al., 2007); Pax6, paired box 6, participates in the cell proliferation and the determination of neuronal fate (Maekawa et al., 2005). Morphologically, NSCs have a prominent process that crosses the granule cell layer (Kriegstein and Alvarez-Buylla, 2009). Apart from their location, RGL cells are distinct from differentiated astrocytes because they are constitutively negative for S-100β, a well established mature astrocyte marker (Steiner at al., 2004). Moreover, mature astrocytes are seldom mitotic in the adult brain in normal conditions (Steiner at al., 2004).

Adult NSCs make up approximately two-thirds of the nestin expressing cells of the SGZ (Kempermann et al., 2004); they are mostly quiescent cells that rest in G_0, with only a small fraction actively progressing through the cell cycle at any given moment. They do not give rise to differentiated cells directly but generate transient-amplifying intermediate progenitor (INPs). Activated RGL cells express the proneural transcription factor (TF) achaete-scute homolog 1 (Ascl1/Mash1), which is induced by neurogenic signals and is specifically required for the exit of stem cells from quiescence (Andersen et al., 2014), indeed its destabilisation by ubiquitination promotes the return of stem cells to a resting state (Urbán et al., 2016). INPs are nestin-positive cells (Filippov et al., 2003) that present a different morphology compared to NSCs: they lack the long process and have cytoplasmatic extensions oriented parallel to the granule cell layer (Fukuda et al., 2004). These proliferating cells start the process of differentiation in which they could become either GFAP-positive or doublecortin-positive (DCX), but never both, indicating two independent cell fates in the glial and neuronal lineages (Steiner et al., 2004). Nestin, which is expressed transiently in adult NSCs and in immature neural progenitor cells, vanishes when differentiation starts. Progenitors committed to the neuronal lineage are characterized by the transient expression of markers such as doublecortin as mentioned before (Brown et al., 2003) (Knoth et al., 2010), and polysialylated neuronal cell adhesion molecule (PSA-NCAM) (Seki and

Arai, 1993). They are also proliferative and keep expressing the stem/progenitor marker Sox2 (Kempermann et al., 2004) (Figure 3).

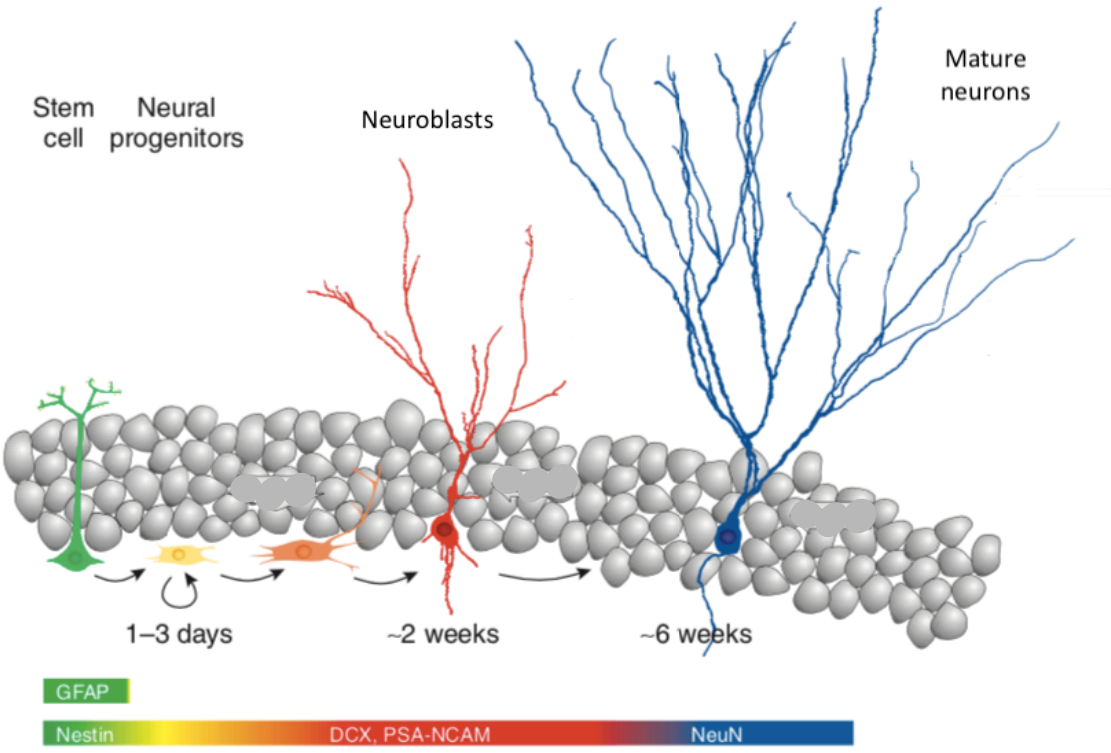

Figure 3. Lineage progression from RGL cell to mature neurone in SGZ, with main proteic markers. Image adapted from *Bischofberger J., 2007.*

Doublecortin is a protein that regulates microtubule polymerization and is expressed in neuroblasts and immature neurons (Brown et al. 2003). It is expressed at very high levels in the prenatal brain and is retained postnatally within the two areas of continuous neurogenesis. The DCX gene was originally described in the context of human cortical disorders: mutant alleles impair migration of neuronal progenitor cells during development and lead to cortical dysplasia (des Portes et al., 1998; Gleeson et al., 1998). As said before, DCX usually co-labels with PSA-NCAM in neuroblasts, and the presence of this cell-to-cell adhesion molecule is correlated with displacement of immature granule cell into the bulk of the GCL and growth of neurites, by reducing cell adhesiveness (Kuhn et al., 1996). DCX expression persists into the next stage, in which the maturing GCs become postmitotic and start expressing young-neuron markers like βIII-tubulin and calretinin, a calcium binding protein. The majority of cells reach this stage in only 3 days after the initial division, and during this time they undergo multiple cycles of replication (Kempermann et al., 2004). In these few days after the first cycle, only from one quarter to one third of these newborn cells, depending on the mouse strain, are able to survive. The number of new cells

stabilises after this dramatic drop, and remains stable over months (Kempermann et al., 2003). Finally, post-mitotic neurons are identified by the presence of neuronal nuclear protein (NeuN), prospero-related homeobox gene 1 (Prox-1), and exchange the expression of calretinin for calbindin (Brandt et al., 2003). NeuN is an early marker of neuronal differentiation that persists in the adult tissue, and it is often used as a marker of postmitotic neurons due to its localization which is predominantly nuclear (Mullen et al., 1992). Prox-1 is a post-mitotic TF required for cell fate specification of DG granule cells, indeed its loss in immature neurones turns them into pyramidal cells of the hippocampus (Iwano et al., 2012) (Figure 3).

From a morphological point of view, NSCs cells undergo an extensive maturation process. Multiple studies (van Praag at al., 2002) (Zhao et al., 2006) performed structural analyses of newborn neurones in the murine DG using a retroviral-based vector expressing a reporter gene that labels the soma, as well as the processes, of proliferating cells only. Thus it was possible to observe newborn neurons integrating in the granule cell layer and, over several months, acquire the morphological and electrophysiological properties of mature granule cells. In particular, in the first week after birth the newborn cell moves a short distance into the inner granule cell layer where it extends limited cellular processes but it is still not integrated into the network; then, after 4 weeks, electrophysiological properties of the new granule cells are indistinguishable from the older ones. However, complete maturation in terms of size of soma, total dendritic length, dendritic branching and spine density, goes on for several months (van Praag at al., 2002). Before the complete integration into the DG circuit, adult-born granule cells have unique characteristics, for example they are hyper-excitable and have enhanced synaptic plasticity. These peculiar features of this population may contribute to specific aspects of learning and memory (Deng et al., 2010)(Schmidt-Hieber et al., 2004).

Neurogenesis in the dentate gyrus is regulated by multiple physiological and environmental signals including adrenal steroids, glutamate receptor activation, multiple growth factors, enriched environmental conditions, exercise, inflammation and antidepressants. These different conditions may affect the behaviour of RGL cells directly or indirectly through the level of neuronal activity within the dentate gyrus. This, in turn, may induce changes in the proliferation rate of these cells and their progeny, as well as the survival of newborn neurones (Kriegstein and Alvarez-Buylla, 2009).

For what concerns regional distributions of neurogenesis, it was reported that the number of proliferative cells can vary between the supra and infra blade of the DG. Specifically, the number of BrdU-labelled cells seems to be significantly higher in the dorsal than in the ventral DG, not immediately after BrdU injections but after some (3 and 6) months. Given the temporal interval, this difference seems a matter of survival of newborn neurons, rather than of proliferation levels (Kempermann et al., 2003).

1.2.3. AHN in learning and memory

The dentate gyrus and the subiculum constitute the hippocampal formation which is critical for certain forms of learning and memory. A positive correlation has been established between neurogenesis in the dentate gyrus and an animal's performance on behavioural tasks.

One of the first studies demonstrated that mice raised in an enriched environment, when compared with mice in standard conditions, show an improvement in spatial-learning tasks assessed in a Morris water maze, together with a higher survival of the progeny of neuronal precursor cells in the hippocampus (Kempermann et al., 1997). A subsequent study demonstrated that among several components of the enriched environment, voluntary wheel running was sufficient to enhance neurogenesis in the adult mouse DG, doubling the number of surviving newborn cells (van Praag et al., 1999). As well as physical exercise, training on associative learning tasks that require the hippocampus, including trace eyeblink conditioning and spatial water-maze training, enhance the number of proliferating cells in the dentate gyrus (Gould et al., 1999b). Although it is not possible to rule out that these stimuli have some effect on cell proliferation, these studies strongly suggest that the increased number of BrdU-labeled cell is mainly due to higher survival rate of new GCs, and not to the proliferation of neuronal precursors. The reasons for this conclusion are that those stimuli increased the number of cells only if animals were injected with BrdU before training, and not during. Second, the number of BrdU-labeled cells was significantly enhanced during the time when the number of new cells is known to diminish in laboratory controls, and this decrease is most likely the result of cell death. Third, a decreased number of pyknotic cells in the SGZ was observed compared to controls (Gould et al., 1999b)(van Praag et al., 1999).

Given the role played by the DG in pattern separation, the possibility that adult born neurones contribute specifically to this hippocampal function has been investigated. Ablating neurogenesis with the use of focal x-irradiation or dominant negative Wnt, impaired performance in

two spatial discrimination tasks when two stimuli were presented with limited spatial separation, but not when two stimuli were widely separated in space. At the same time, these mice were not impaired at the hippocampus-dependent paired-association-learning task, indicating that they are able to learn complex object-place associations even at reduced levels of neurogenesis (Clelland et al., 2009). The same result was confirmed in another study in which survival of adult newborn neurones was enhanced in mice by a conditional knock-out of the pro-apoptotic gene *Bax* in nestin^{+} cells. These mice showed normal behaviour in several cognitive tasks but were more efficient in differentiating between overlapping contextual representations, which is indicative of enhanced pattern separation (Sahay et al., 2011). Furthermore, stimulation of adult hippocampal neurogenesis with *Bax* KO combined with voluntary exercise, produced a marked increase in exploratory behaviours and decreased anxiety-like behaviours. However, in this specific case, the number of newborn neurones in mice after exercise was not higher than in control mice. Therefore, this results may be explained by enhanced properties of the already present excitable young newborn neurones (Sahay et al., 2011).

1.2.4. AHN in humans

The frequency, location and function of adult neurogenesis in humans is still debated. Indeed, measuring neurogenesis in humans is considerably more difficult.

The first time that proliferating cells were detected in the human brain was with the study of Eriksson et al. in 1998. This research group used postmortem tissue from cancer patients that were injected with BrdU for diagnostic purposes. In this setting they showed the presence of proliferating cells in both the SVZ and SGZ, and they found evidence for postnatal neurogenesis demonstrating that a fraction of BrdU-positive cells colabelled with markers of mature neurones NeuN, calbindin and neuron specific enolase (NSE) (Eriksson et al., 1998). BrdU is the gold standard for detection of proliferating cells, and also for investigation of fate choices and rates of neurogenesis. However, as BrdU is a compound formerly developed to radiosensitise cancer cells since its incorporation weakens the DNA strand, it may be toxic at high doses and therefore its use in humans is limited for ethical reasons (Curtis et al., 2011)(Gault and Szele, 2021).

The pool of patients considered in the study of Eriksson et al. was quite low: 5 patents with the oldest one at 72 years of age. Nevertheless, it was followed after some years by an extensive study of 54 human samples ranging in age from 1 day to 100 years (Knoth et al., 2010). In this case,

researchers first validated doublecortin as marker of human granule cell development in fetal tissues, then used immunohistochemical techniques on postmortem tissues and showed the presence of DCX-positive cells in every sample. The proliferating nature of these neuroblasts was confirmed with double labelling with markers of proliferation (Ki67, Mcm2 and PCNA). Additionally, researchers confirmed the neuronal nature of these cells by combination of DCX labelling with several markers of neural differentiation, e.g. nestin, PSA-NCAM, Sox2, Prox1, β-III-tubulin, NeuN, and calretinin, and finding co-labelled cells for each of them, confirming data found until then in rodents. Finally, they found an age-related reduction of the amount of DCX-positive cells (Knoth et al., 2010).

However, in most recent years other studies based on immunohistochemical detection of markers of neurogenesis, reported contrasting evidence. They reported that proliferation in the human DG is undetectable during childhood (Dennis et al., 2016); moreover, they did not observe DCX^+ $PSA\text{-}NCAM^+$ neuroblasts in the SGZ in any of the tissues analysed, from the second to the eighth decade of life (Sorrells et al., 2018). Conversely, in another study published at the same time, researcher observed DCX^+ $PSA\text{-}NCAM^+$ cells in the SGZ of individuals from 14 to 79 years of age, and in comparable numbers (Boldrini et al., 2018). Further studies support these findings: Llorens-Martin's group detected DCX^+ neurons in the DG up to the ninth decade of human life, with a density of 25.000 cells/mm^3 ca in the entire dentate gyrus (Moreno-Jiménez et al., 2019). The majority of the DCX^+ cells co-expressed Prox1 and other neuronal markers, such as NeuN, while a subset of these cells co-labelled with more immature markers such as PSA-NCAM. In a subsequent study, the same team found the same density of DCX^+ cells in another cohort of health subjects, however they never demonstrated them to be positive for Phospho-Histone 3 (PH3), the proliferative marker that was used in the study (Terreros-Roncal et al., 2021); for this reason the proof of neuroblasts proliferative capacity can not be considered consistent (Gault and Szele, 2021). Additionally, Llorens-Martin's studies demonstrated the presence of cells positive for nestin, GFAP, Sox2 and vimentin in the SGZ of some healthy patients, with morphological characteristics of NSCs. Also in this case there was no evidence of these RGL cells being in S phase (Terreros-Roncal et al., 2021). In this regard, Boldrini et al. showed images of $Nestin^+$ cells co-labelled with Ki-67 in SGZ proving at least qualitatively the possibility to find mitotic RGL cells (Boldrini et al., 2018).

The first study by Llorens-Martin et al. was published together with a state-of-the-art protocol paper that accurately describes all the steps in performing immunohistochemistry on

human brain tissues. They describe every procedure from collection of samples by pathologists to image analysis, and compares times of tissue collection (post-mortem delay PMD), methodology and timing of tissue fixation, as well as variations of histological protocols, and their effect on the performance of several antibodies anti-markers of neurogenesis (Flor-García et al. 2020). The main finding regarding the methodology was that over-fixation of the tissue leads to a drastic reduction of DCX^+ immunodetection (Gault and Szele, 2021). They showed that detectable DCX levels are reduced after 12h of fixation and the epitope is masked after 24h of fixation, but with no effect in case of post mortem delay up to 38h. In general, this study defines a series of parameters to take into account and that should be reported when working with human brain tissues for immunohistochemical analysis of neurogenesis, in order to increase data reproducibility between laboratories. With these considerations in mind, we could explain the aforementioned conflicting results on the presence of neuroblasts in SGZ, with differences in materials and methods employed: in Sorrells et al., tissues had a PMD up to 48 h, and in Dennis et al., some samples had PMD up to 90 h (Gault and Szele, 2021).

In general, the inconsistency of these results highlights the need for additional ways to study the generation of new neurones in adult humans. An interesting approach was proposed in 2013 by Spalding et al. based on the content of carbon-14 in genomic DNA of hippocampal cells in humans. This strategy takes advantage of the elevated atmospheric ^{14}C levels caused by nuclear bomb testing between 1955 and 1963 during the Cold War. With this system and through a mathematical model that allows retrospective birthdating, researchers showed evidence for human neurogenesis in the SGZ, with an annual turnover of 1.75% of hippocampal neurones (Spalding et al., 2013). The study takes into consideration the integration of ^{14}C after DNA damage and repair in non-proliferating cells. However, the amount of radiocarbon detected in other regions of the brain like the cerebral cortex, cerebellum and olfactory bulb, and in neurons surviving at the perimeter of an ischemic cortical stroke, a situation where there is substantial DNA damage and repair, is not comparable with the concentrations found in the hippocampal region. Thus, their data are likely to reflect the process of neurogenesis.

This year, thanks to recent advances in single-cell transcriptomics, the single-nucleus RNA sequencing technique has been applied with the aim of identifying the existence, abundance and molecular properties of immature neurones in the adult human hippocampus (Zhou et al., 2022). A machine learning-based approach, pre-trained on human infant hippocampal specimens, allowed the

identification of immature neurones DCX^{+}PROX1^{+}CALB1- specifically in the cluster of granule cells, across all ages (from few months to 88 years of age). Additionally, quantitative measurements were obtained from several hippocampal datasets showing that the percentages of immature GCs decreases with age. Transcriptomic analysis can not tell us whether these immature neurons were born late in life or born earlier and remained in the immature state, hence the implementation of an *ex vivo* human dentate gyrus slice culture. Fresh surgically resected tissues can be cultured and adding EdU to the medium it was possible to observe the presence of proliferating DCX^{+}PROX1^{+} cells, demonstrating with another methodology the capacity for the adult human dentate gyrus to generate new GCs (Zhou et al., 2022). Comparison of the molecular signature of human and murine cells is relevant for the field: in the transcriptomic landscape of human immature granule cells across all ages, only 15.5% of genes overlap with orthologous genes enriched in mouse immature GCs across ages. This finding highlights a substantial interspecies difference that should be taken into consideration when translating studies from rodents to humans (Zhou et al.. 2022).

1.3. Subventricular zone

The other neurogenic niche in the adult mammalian brain is the the subventricular zone. The SVZ is a layer of cells extending along the striatal and septal walls of the lateral ventricles, that harbours NSCs that give rise to neurons that migrate into the olfactory bulb. A single layer of multi-ciliated ependymal cells separates the SVZ from the lateral ventricle (Lazarov et al., 2010).

Similar to the SGZ, putative NSCs found in the SVZ are quiescent, GFAP-positive cells that share properties of astrocytes and are referred to as type B cells. These cells give rise to transit-amplifying type C cells that are GFAP-negative (Lim and Alvarez-Buylla, 2016). These intermediate progenitor cells give rise to PSA-NCAM and DCX-expressing neuroblasts, or type A cells, that migrate in chains from the LV, through the rostral migratory stream towards and then into the olfactory bulb, where they differentiate into either granule cells or periglomerular neurons (Doetsch and Alvarez-Buylla, 1996). As for RGL cells in SGZ, type B cells also give rise to glial lineages, including oligodendrocytes and nonneurogenic astrocytes. Estimates indicate that thousands of new OB neurons are generated every day in the young adult rodent brain (Lim and Alvarez-Buylla, 2016).

The adult human SVZ has a very different cellular organization to the one observed in rodents. Very few cells with the morphology and marker expression of migrating young neurons

have been observed in human tissue, and migration from the neurogenic niche to the OB, is rare, or nonexistent (Lim and Alvarez-Buylla, 2016). Nevertheless, the rodent SVZ remains an appealing model for the cellular and molecular investigation of neurogenesis and postnatal human brain development, as well as for the understanding of the origin of brain tumors (Lim and Alvarez-Buylla, 2016).

2. Alzheimer's disease

Alzheimer's disease is a condition characterized by loss of memory and cognition, hence the hippocampus is of great interest in this field. Since the dentate gyrus is one of the areas that continues to generate newborn cells throughout life as discussed above, and AHN has been associated with memory and learning, SGZ neurogenesis may have a role in AD progression.

Dr. Alois Alzheimer was the first to observe the disease named after him in 1901, in a 51 year old woman who experienced memory impairment and disorientation. In the postmortem analysis of the brain tissues, the doctor reported peculiar changes in the neurofibrils and a high concentration of protein plaques in the cortex. This was the first time the major hallmarks of AD pathology were described (Neurobiology of Brain Disorders, 2014). AD is the most common cause of dementia: it accounts for an estimated 60 to 80 percent of cases. Autopsy studies show that less than half of these cases solely involve Alzheimer's pathology, the majority are mixed dementias, and the most often associated pathologies are vascular and Lewy body dementia (2022 Alzheimer's disease facts and figures). Brain changes associated with Alzheimer's may begin 20 or more years before symptoms appear. The symptoms change over years, reflecting the degree of damage to neurons in different parts of the brain. When initial changes occur, the brain compensates for them, enabling individuals to continue to function independently in many areas. However, as neuronal damage increases, the brain can no longer compensate for the changes and individuals show cognitive decline, and are likely to require assistance with activities for safety reasons. In the moderate stage, which for some is the longest, neuronal damage is so significant that individuals start showing severe symptoms. They may have difficulty performing routine tasks, become confused about where they are and begin wandering, and start having personality and behavioural changes, including suspiciousness and agitation. They may also begin to have problems recognizing loved ones. In the severe stage, patients require help with basic activities of daily living. Because of

damage to areas of the brain involved in movement, individuals become bed-bound, a condition that makes them vulnerable to blood clots, skin infections and sepsis, all conditions that can ultimately be fatal. Damage to areas of the brain that control swallowing makes it difficult to eat and drink, and this increases the risk for swallow food into the trachea. Food particles deposited in the lungs can cause aspiration pneumonia, which is a significant cause of death among many individuals with Alzheimer's (2022 Alzheimer's disease facts and figures).

2.1. Epidemiology

More than 25 million people in the world are currently affected by dementia, most suffering from AD, with around 5 million new cases occurring every year. 6.5 million Americans age 65 and older are estimated to be living with Alzheimer's dementia. Aging is the strongest risk factor for AD; indeed, the percentage of people with AD increases with age (2022 Alzheimer's disease facts and figures).

AD has a sex-biased epidemiological profile, affecting approximately twice as many women as men. The higher frequency of the pathology observed in women compared to men, may be partially explained by the fact that women live longer on average, since age is the greatest risk factor for Alzheimer's. However, differences in longevity alone cannot explain the fact that around two-thirds of affected individuals are women (Snyder et al., 2016). Genome-wide association studies have detected AD-associated loci that are sex specific, indicating sex disparities in the genetic basis of the pathology (Peeters et al., 2021, Nazarian et al., 2019). Even sex hormones are thought to play important roles linked to sex vulnerability to aging and AD. Both estrogen and androgens have been demonstrated to be protective against neuronal degeneration, and although both sexes experience hormonal declines in midlife, the decrease of estrogen levels in women is more abrupt, resulting in a greater risk of AD. (Snyder et al. 2016, Peeters et al. 2021) Sex/gender differences in lifestyle-related AD risk factors, such as diet, physical activity and education, may also contribute to differences in AD incidence (Snyder et al. 2016, Peeters et al. 2021).

2.2. Pathology

There are no macroscopic changes specific for Alzheimer's pathology. Nevertheless, brain cortical atrophy is often detected in AD patients: the frontal and temporal cerebral cortices present enlarged sulcal spaces with atrophy of the gyri. Indeed, medial temporal atrophy affecting the

amygdala and hippocampus is typical of AD, usually accompanied by enlargement of the temporal horn of the lateral ventricles. (DeTure and Dickson, 2019).

The microscopic characteristics of AD neuropathology are progressive intracellular and extracellular accumulations of insoluble fibrous material. Firstly, abnormally phosphorylated tau assembles into paired helical filaments that aggregate into neurofibrillary tangles (NFTs) in the neuronal perikarya and dystrophic neurites. The second pathological hallmark is the extracellular deposition of amyloid-β peptides, forming diffuse and neuritic senile plaques (Neurobiology of Brain Disorders, 2014). Indeed, this deposited material is not distributed randomly in brain areas but shows a characteristic pattern (Braak and Braak, 1995). The result of these lesions is the loss of synapses and neurons in vulnerable regions of the brain, leading to the symptoms commonly associated with AD. Evidence suggests that amyloid deposition and tau pathology in AD precede structural changes in the brain, including hippocampal volume loss and decreased glucose metabolism (DeTure and Dickson, 2019).

2.2.1. Molecular biology of AD

Aβ peptides are generated in the so-called amyloidogenic pathway through sequential proteolytic cleavage of the type-1 transmembrane amyloid precursor protein (APP). APP is expressed in many tissues, especially in the synapses of neurons. It has been implicated as a regulator of synaptic formation and repair, anterograde neuronal transport and iron export; however, deletion of APP in mice produces very little phenotype and does not suggest that a loss of APP or Aβ function is deleterious to the adult animal (O'Brien and Wong, 2011). APP consists of a single membrane-spanning domain, a large extracellular glycosylated N-terminus and a shorter cytoplasmic C-terminus (Chen et al., 2017). APP is produced as several different isoforms, ranging in size from 695 to 770 amino acids, that are expressed differentially by tissue type. The most abundant form in the brain (APP695) is produced mainly by neurons, whereas APP751 and APP770 are mainly expressed in the peripheral nervous system and by platelets (Chen et al., 2017).

APP is produced as a precursor molecule processed by two secretases: the aspartyl protease β-site APP cleaving enzyme 1 (BACE1, also termed β-secretase) and the tetrameric γ-secretase complex. β-secretase can cleave APP at two alternative sites, either at Asp_1 or at Glu_{11} of the Ab sequence, leading to the generation of a 99 aa C-terminal fragment (CTF or C99) or a 89 aa CTF (or C89) that will then be further processed by γ-secretase to full-length $Abeta_{1-x}$ or the N-terminally

truncated $Ab_{11\text{-}x}$, respectively (Siegel et al., 2017). C99 and C89 generated by β-secretase cleavage, can be internalized and further processed by γ-secretase at multiple sites to produce cleavage fragments that contain between 37 and 49 amino acids that are further cleaved to the main final Aβ forms, $Aβ_{1\text{-}40,42}$ and $Aβ_{11\text{-}40,42}$ (Chen et al., 2017). The cleavage by γ-secretase also liberates an APP intracellular domain (AICD) that translocates into the nucleus, where it regulates gene expression, including the induction of apoptotic genes (Greenwood et al., 2022). Production of these Aβ forms is precluded if APP is processed by α-secretase that cleaves within the Aβ sequence. This cleavage releases sAPPα from the cell surface and leaves an 83-amino-acid C-terminal APP fragment (C83). C83 is subsequently processed by γ-secretase, releasing the P3 peptide and AICD (Siegel et al., 2017) (Figure 4).

The γ-secretase membrane multiprotein complex is composed of presenilin 1 (PS1) or presenilin 2 (PS2), nicastrin, presenilin enhancer 2, and anterior pharynx defective 1. This complex cleaves many type-I transmembrane proteins, including APP and Notch (Bergmans and De Strooper, 2010). PS1 and PS2 are the transmembrane proteins that form the catalytic core of the γ-secretase complex. PS2 is expressed in a variety of tissues, including the brain, where it is expressed primarily in neurons (Bekris et al., 2010, Bergmans and De Strooper, 2010).

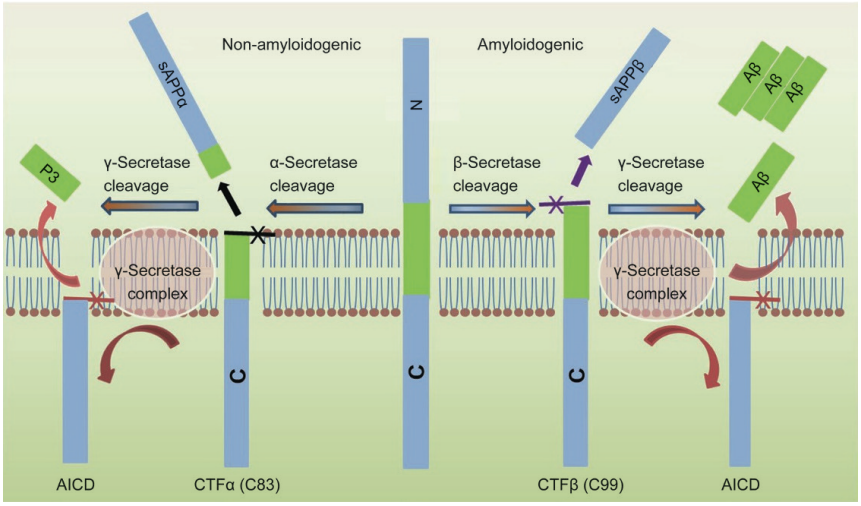

Figure 4. Human APP proteolytic pathways. From *Chen et al. 2017.*

2.2.2. Amyloid plaques

The major component of amyloid plaques, as the name suggests, is Aβ. The most common form of Aβ in humans is 40 amino acids long, whereas $Aβ_{42}$ is less common, occurring in about ten

percent of $A\beta_{40}$, but is considered to be pathogenic (Bergmans and De Strooper, 2010). Additional Aβ peptides containing between 38 and 43 amino acids are also detected, but $A\beta_{42}$ is the most fibrillogenic and the predominant component of amyloid plaques. Aβ peptides adopt β-sheet secondary structures assembling first into protofilaments and finally into fibrils. Amyloid fibrils are larger and insoluble, and they can further assemble into amyloid plaques (Chen et al., 2017). However there is no direct correlation between amyloid plaque burden and the loss of synapses and neurons in AD (Hsia et al., 1999), instead the amount of oligomeric Aβ is increased in AD brain extracts. These findings led to the hypothesis that soluble Aβ oligomers exhibit greater toxicity than insoluble fibrils or plaques, and trigger synapse failure (Mucke et al., 2000). The main feature of oligomers is the solubility, which allows these spherical particles to spread throughout the brain and with the cell membrane, causing cell death (Chen et al., 2017).

The two types of amyloid plaques most commonly observed in AD are diffuse plaques and dense core plaques. Diffuse plaques are stained weakly by amyloid binding dyes, and they do not trigger accumulation of activated microglia and reactive astrocytes. Conversely, dense core plaques present a compact amyloid formation and are intensely positive with thioflavin S and Congo red, suggesting they contain more fibrillogenic forms of Aβ. More importantly, a subset of dense core plaques have neuritic elements, and these neuritic plaques (NPs) are closely associated with neuronal loss and cognitive decline in AD (DeTure and Dickson, 2019). This is explained by a model in which APP and proamyloidogenic secretases are transported to neurons terminals from where Aβ peptides are released; the increasing accumulation of $A\beta_{42}$ at terminals forms these NPs and synaptic function are disrupted. Microglia cells and, less frequently, reactive astrocytes, surround amyloid plaques and produce cytokines, chemokines, and other inflammatory factors that may increase the damage to neuronal circuits (Neurobiology of Brain disorders, 2014).

2.2.3. Neurofibrillary tangles

Neurons bearing neurofibrillary tangles (NFTs) are another frequent finding in AD brains, and the temporal and spatial appearance of these tangles more closely reflects disease severity than does the presence of amyloid plaques (Braak and Braak, 1995).

Tangles are fibrillary intracytoplasmatic inclusions formed by hyperphosphorylated tau, a microtubule-associated protein, which in this state aggregates in an insoluble form. Normally, tau is

transported anterogradly in axons where it helps stabilizing microtubules. In AD instead, tau proteins are hyperphosphorylated and abnormally folded compared to unassembled normal tau, and they lose their normal ability to bind microtubules (DeTure and Dickson, 2019). This loss of tau function is coupled with increased aggregation properties for abnormal tau. Evidence suggests that tau behaves in a "prion-like" manner, and that seeding and spreading of pathological tau drives progressive neurodegeneration (Sala-Jarque et al., 2022). NFTs develop from intracellular misfolded tau and are found in the cell body and in proximal dendrites of affected neurons. Abnormal protein aggregates can also be found in neuropil threads (NTs) which are dendritic and axonal elements containing filamentous tau. After death of the parent cell, the NFT converts into an extraneuronal structure called "ghost tangle", eventually becoming engulfed and degraded by glial cells (Braak and Braak, 1988).

2.2.4. Distribution of lesions

In AD, amyloid plaque and neurofibrillary tangle formation tend to form in neuroanatomically stereotypic patterns. The region-specific formation of the lesion, which evolves in time, has led to several staging schemes.

Amyloid plaques are irregularly distributed and, therefore, do not represent a useful tool for the differentiation of progressive stages of the pathology. NFTs and NTs generally show a hierarchical and highly characteristic pattern of distribution with only minor inter-individual variations (Braak and Braak, 1991). Therefore, on tangles is based the most widely used staging scheme proposed in 1991 by Heiko and Eva Braak. The first region to experience neurofibrillary pathology is the transentorhinal region (TR), which is a complex transition zone located between the proper entorhinal region and the adjacent temporal isocortex (Stage I). Then NFTs extend into layer II of the entorhinal cortex (Stage II), and proceed to the hippocampus CA1 region, subiculm and temporal neocortex (Stage III). Afterwards the lesions spread to the rest of the hippocampal formation (Stage IV), isocortex (Stages V) and primary sensory areas (Stage VI) (Braak and Braak, 1995)(Figure 5).

The presence and pattern of lesions, correlates with neuronal loss which is a basic and fundamental feature in the pathogenesis of AD. Nevertheless, the pathological mechanisms leading to neuronal death, as well as the reasons for selective susceptibility of specific neuronal population, are still to be elucidated. Neurons that are vulnerable to the accumulation of pathological forms of

tau and that are lost early in the disease, mainly include large pyramidal neurons in layer II of the entorhinal cortex (EC), the subiculum, the CA1 region of the hippocampus, corticopetal cholinergic neurons in the basal forebrain, and noradrenergic neurons in the locus coeruleus (Fu et al., 2018). Memory loss and dementia are primarily attributed to the loss of neurons in the cortex and the hippocampus. Nevertheless, atrophy of the presubiculum and subiculum are the earliest hippocampal anatomical markers of AD, which reflects the severe degeneration of the perforant pathway penetrating the hippocampal formation through the subicular field. (Carlesimo et al., 2015).

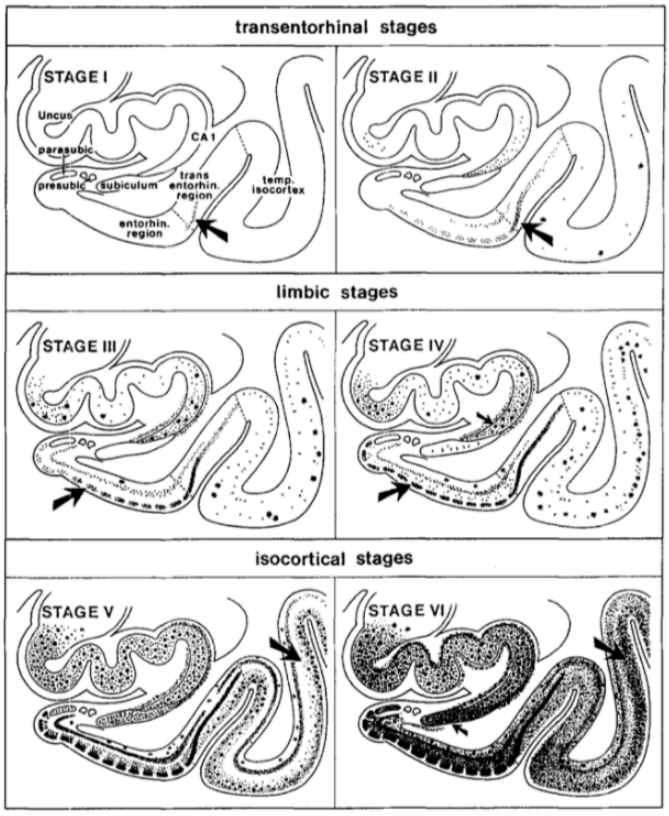

Figure 5. Braak staging of AD-related neurofibrillary changes. From *Braak and Braak, 1995.*

2.2.5. Neuroinflammation

Even though both Aβ and tau deposition are AD hallmarks, it is debated whether they initiate AD pathology. Other factors are considered to contribute to the pathology. Nevertheless, the discovery of increased levels of inflammatory markers in patients with AD and the identification of AD risk genes associated with innate immune functions, suggest that neuroinflammation has a prominent role in the pathogenesis of AD.

Neuroinflammation generally refers to an inflammatory response within the CNS that can be caused by various pathological insults. In the process, innate immune cells of the CNS produce pro-inflammatory cytokines, chemokines, small-molecule messengers, and reactive oxygen species

(Leng and Edison, 2020). These released molecules can lead to synaptic dysfunction and neuronal death. In the context of neurodegenerative disease, neuroinflammation tends to be a chronic process that fails to resolve by itself and is considered a vital driver of the disease. Among glial cells, microglia are considered the main source of proinflammatory molecules within the brain (Heneka et al., 2015). In presence of an endogenous or exogenous pathological insult, microglial surface receptors can recognize pathogens, cell debris or abnormal proteins and induce internalization through various endocytic pathways (Leng and Edison, 2020). At the same time, microglia contribute to the protection and remodeling of synapses for proper maintenance and plasticity of neuronal circuits (Heneka et al. 2015). In AD, microglia are able to bind to soluble Aβ oligomers and Aβ fibrils via receptors, and engulf them by phagocytosis. In sporadic cases of AD, inefficient clearance of Aβ by phagocytosis and resulting persistent activation of microglia, has been identified as a major pathogenic pathway (Leng and Edison, 2020). Single-cell transcriptomic studies in mouse models of AD, have shown that disease progression is paralleled in microglia by a gradual transition from a homeostatic state to a disease-associated state (Disease Associated Microglia, DAM). The transition to DAM is coupled with downregulation of homeostatic genes and elevation of lipid metabolism pathways and phagocytic-related genes, corresponding to the need for plaque clearance. In addition, loss-of-function mutations of the DAM-upregulated genes are known to be linked to elevated risk of developing AD, e.g. triggering receptor expressed on myeloid cells 2 (*TREM2*) (Keren-Shaul et al., 2017). It was also demonstrated that DAM are mainly localized in the vicinity of Aβ plaques. Moreover, it has been proven that this cell population is conserved in humans by single-cell genomic analysis and immunohistochemistry of post-mortem AD brains (Keren-Shaul et al. 2017).

This neuroinflammatory process is a response to the presence of protein aggregates and neuronal loss. However, sustained neuroinflammation from the early stages of AD exacerbate the generation of Aβ and NFT and worsens neuronal toxicity and death contributing to the progression of the pathology.

2.3. Familial Alzheimer's disease

A small percentage of Alzheimer's cases, less than 1%, present an autosomal dominant inheritance. This rare form the pathology is called familial AD (FAD) and affected individuals tend to develop symptoms before age 65, sometimes as young as age 20. In general, early-onset

Alzheimer's disease (EOAD) defines the form of the pathology arsing before age 65 and though it is slightly more common than FAD, its cases account for fewer than 5% of the diagnosed AD cases.

FAD develops as a result of mutations in any of three specific genes. These inherited mutations involve the gene for the amyloid precursor protein (APP) and the genes PSEN1 coding for the presenilin 1 protein and PSEN2 for presenilin 2 protein. These genes influence the same biochemical pathway, namely the production of Aβ species (DeTure and Dickson, 2019). Mutations in PSEN1 are the most common cause of familial AD: they result in a change in presenilin 1 function that lead to reduced γ-secretase activity which in turn increases the ratio of Aβ42 to Aβ40. In contrast, missense mutations in the PSEN2 gene are rare, explaining <1% of EOAD patients (DeTure and Dickson, 2019). However, the result of PSEN2-associated mutations is the same, namely an increase in the ratio of Aβ42 to Aβ40. The same is true for pathogenic mutations in APP that account for <1% of EOAD patients (DeTure and Dickson, 2019). Most of the pathogenic missense mutations affect APP processing and are located near the β- or γ-secretase cleavage sites. These mutations result in overproduction of either total Aβ, such as the Swedish mutation, or a shift in the Aβ40/Aβ42 ratio toward the more toxic Aβ42 peptide, as occurs with the Florida mutation and the London mutation (Hoogmartens et al., 2021).

2.5. Late-onset Alzheimer's disease

Late-onset AD (LOAD) represents the vast majority of AD cases and it is defined as disease appearing after 65 years of age. This form of the pathology is not linked to causative mutations and indicates that the aetiology of the disease is more complex than seen for FAD.

The biggest risk factor for LOAD is older age, in addition to having a family history of the pathology. This form of the disease is considered sporadic, however genetic risk factors have been identified, most notably the apolipoprotein E gene (*APOE*). The human *APOE* gene exists as three polymorphic alleles ε2, ε3 and ε4. Individuals carrying a single copy of the *APOE-ε4* polymorphism have a 3-fold increased risk compared to non-carriers, those homozygous have a 12-fold increase, whereas carriers of ε2 polymorphism have a decreased risk. In addition, those with the ε4 form are more likely to develop Alzheimer's at a younger age than those with the ε2 or ε3 forms (Corder et al., 1993). Differences between the three ApoE isoforms are limited to amino acid residues 112 and 158. The single amino acid differences at these two positions affect the structure of the protein and influence its ability to bind lipids, receptors and Aβ (Liu et al. 2013). In fact,

ApoE is a transport protein that regulates lipid homeostasis by mediating lipid transport from one tissue or cell type to another. In the CNS, ApoE is mainly released by astrocytes into the interstitial fluid (ISF) of the brain, and transports cholesterol to neurons through members of the low-density lipoprotein receptor (LDLR) family (Liu et al., 2013). ApoE also interacts with Aβ and mediates its clearance via ApoE receptors LRP1, LDLR and VLDLR, which are widely expressed in neurons, astrocytes and microglia, as well as in endothelial cells, astrocytes and smooth muscle cells at the blood-brain-barrier (BBB) and cerebral arteries. Indeed, Aβ is cleared from the brain by receptor-mediated endocytosis in the brain parenchyma, along with the interstitial fluid drainage pathway or through the BBB (Bu, 2009). *APOE*ε4 polymorphism can impair Aβ clearance triggering formation of Aβ oligomer which are in fact more abundant in *APOE*ε4 carriers than in non carriers (Schmechel et al., 1993). Additionally, Aβ binding to ApoE compromises its lipid-binding function, therefore a malfunction of the neuronal cholesterol metabolism is thought to be a causal factor in Alzheimer's disease (Chen et al., 2017) Moreover, *APOE*ε4 shows an association with cerebral amyloid angiopathy (CAA), which refers to the pathological condition in which amyloid spreads and deposits throughout the cerebral blood vessel walls (Liu et al., 2013).

The increased risk associated with having a family history of Alzheimer's is not entirely explained by inheritance of the *APOEε4* risk gene. Other risk factors for LOAD are now known. A recent genome-wide association studies (GWAS) report 38 risk loci (Wightman et al., 2021), that not only affect APP and tau directly, but also modulate cholesterol metabolism (E.g. *APOE*, *ACAB7*), endocytosis (E.g. *CLU*) and immune response (E.g. *TREM2*), mainly encoding for cell-surface receptors involved in the response to the pathological progression.

2.5. Animal models of AD

Modelling AD, as well as all the pathologies associated with aging, represents a challenge. Nevertheless, current models of AD are mainly restricted to transgenic mice with AD-related pathology caused by specific mutations present in early-onset familial AD.

Several transgenic mouse models have been developed to recapitulate features of FAD, and they model predominantly Aβ amyloidosis. These animals harbour mutated human APP, PS1 and PS2 transgene, and they range from mice carrying a single mutated gene to complex triple transgenic animals. Tg APP-based models overexpress the human gene bearing human FAD mutations; the most commonly used are the Swedish mutations (APPK670N and M671L), and the

"London" mutation (APPV717I) which cause an increase in Aβ production (Sanchez-Varo et al., 2022). Tg mice expressing familiar mutations in either PS1 or PS2 present an altered processing of murine APP, however they do not develop plaques, confirming that the expression of human APP is absolutely required to reproduce Aβ deposition in mice. Once these aspects had been considered, a new generation of double Tg mice co-expressing mutations in human APP and PS1 or PS2 was produced. Among them, the most used strains are the APPswe/PS1dE9, APP751SL/PS1M146L and 5xFAD mice. In general, these models develop an accelerated and more aggressive amyloidosis, accompanied by an earlier appearance of cognitive and histopathological AD hallmarks (Sanchez-Varo et al., 2022).

However, the modelling of the second hallmark of AD, NFTs, proved be more complicated. Indeed, APP-models are able to generate hyperphosphorylated tau, but not intracellular NFTs. Only the incorporation of mutant human MAPT transgenes allowed the study of the interaction between the two proteinopathies *in vivo* (Sanchez-Varo et al. 2022). However, we know that these mutations are linked to frontotemporal dementia with parkinsonism and not AD. Additionally, another important limitation is that most of the available tau Tg mice do not reproduce the characteristic progression pattern of NFTs seen in AD patients.

2.5.1. 5xFAD

In order to create a very rapid AD amyloid model, a transgenic mouse that coexpresses a total of five FAD mutations was developed by Oakley et al. in 2006. It harbours 5 mutations inserted in 2 human transgenes involved in the pathology: in APP the Swedish K670N/M671L, Florida I716V, and London V717I mutations and in PS1 M146L and L286V mutations. Transgenic lines were produced by pronuclear coinjection of APP and PS1 transgenes in C57/B6XSJL hybrid embryos, each using the neuron-specific mouse *Thy1* promoter to drive overexpression in the brain. All transgenes were inserted at a single locus where they have been proven to not affect any known gene (Oakley et al., 2006). The line is maintained hemizygous for the transgenes on a C57Bl/6J background.

The main advantage of the 5xFAD mouse model is the rapid amyloid plaque formation that is seen in mice as young as 2 months of age, unlike most AD mouse models that develop plaques only after 6 or more months of age. Intraneuronal Aβ accumulation has also been observed before the formation of plaques at 1.5 months of age. Amyloid plaques first appear in layer V of the cortex

and in the subiculum and by six months plaques are found throughout the hippocampus and cortex by six months. In older mice, plaques are present in the thalamus, brainstem, and olfactory bulb, but are absent from the cerebellum. 5XFAD lines also exhibit astrogliosis and microgliosis beginning at around two months of age, developing in parallel with amyloid deposition. Indeed, this model recapitulates degeneration of synapses and neuronal loss which occurs in multiple brain regions, beginning at about 6 months in the areas with the most pronounced amyloidosis. 5XFAD mice display a range of cognitive and motor deficits, in particular hippocampus-dependent spatial working memory by 4 –5 months of age is significantly impaired as tested in Y-maze tests and cross-maze test (Oakley et al., 2006) (Figure 6).

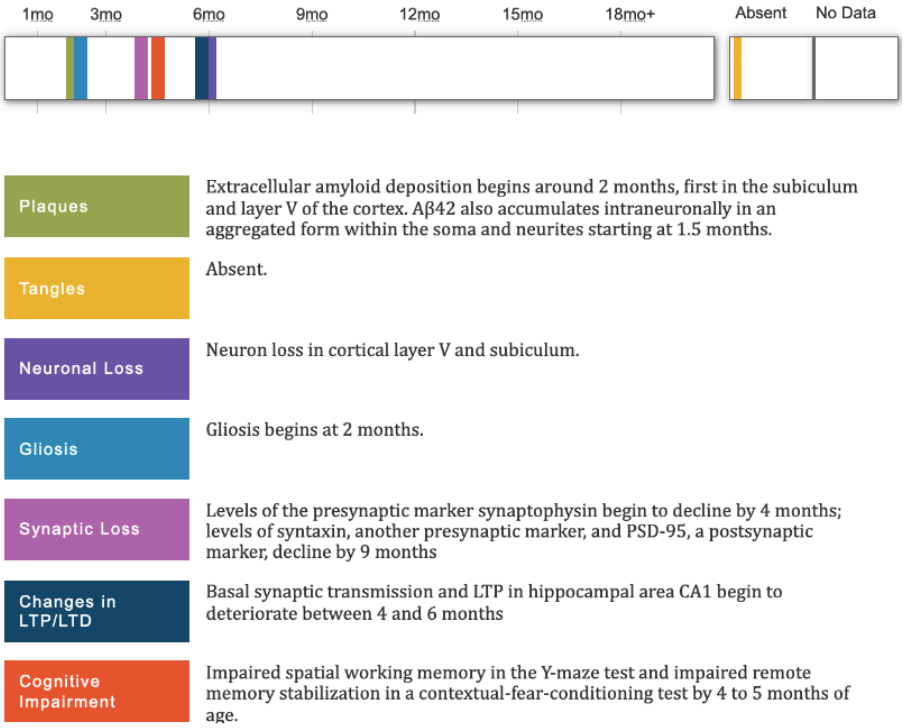

Figure 6. Phenotype characterization and progression of disease in 5xFAD mice. From *www.alzforum.org*

Another relevant aspect to be considered when employing 5xFAD mice, is that amyloid pathology is more severe in females than in males: females express more APP than males and show greater plaque deposition (Oakley et al., 2006). This is probably due to an estrogen response element in the *Thy1* promoter that is used to drive transgene expression (Oblak et al., 2021). Another significant sex-based difference is the elevated level of cholesterol in female 5XFAD and also in wild type females C57Bl/6J mice, compared to males. This aspect seems to recapitulate gender-biased cholesterol levels that are known to differ in humans, and this is quite relevant since pathways involving cholesterol levels may play a role in AD development (Oblak et al., 2021).

As the 5XFAD mouse model was originally designed for the investigation of Aβ-related pathology, it is not expected to develop tauopathy. However, recent studies revealed that 5xFAD mice display a significant aggregated p-tau stained by thiofalvin S and by monoclonal antibody AT8 (Shin et al., 2021). More in-depth studies are required to better characterize these p-tau aggregates, nevertheless their presence opens new possibilities for the investigation of causal events guiding the emergence and progression of FAD.

3. AHN in Alzheimer's disease

Alzheimer's disease is characterized mainly by symptoms like loss of memory and cognition, and AHN has been associated with memory and learning. As a consequence, SGZ neurogenesis has been consider and studied in AD progression.

Declines in hippocampal-dependent spatial memory and pattern separation impairments have been correlated to normal ageing in rodents (Sahay et al., 2011)(Creer at al., 2010), and decreases in neurogenesis levels have been associated with senescence. This last observation has been explained by different models. Specifically, an age-dependent reduction in proliferation levels was observed since the first publications regarding AHN (Altman et al., 1965), but also a decrease in the survival rate of newborn neurones has been proven (Kempermann et al., 1998). Also the pool of quiescent NSCs significantly decreases with age, possibly due to a conversion of adult neural stem cells into astrocytes (Encinas et al., 2011). Another aspect that may explain lower levels of neurogenesis, is the progressively longer time spent by stem cells in quiescence during aging (Ziebell et al., 2018). Additionally, it has been demonstrated that aging mice subjected to events that can boost neurogenesis, such as running, present an improved performance at spatial pattern separation tasks compared to control animals (Creer et al., 2010), as well as an increase in rates of survival of newborn neurones (van Praag et al., 2005).

The decline in neurogenesis that occurs in physiological aging is exacerbated in neurodegenerative diseases, including AD. Indeed, aging is also the greatest risk factor for Alzheimer's disease. Impairments in neurogenesis have been described extensively in animal models of AD (Li Puma et al., 2021). When comparing these studies there seems to be a huge variability, depending on age of the animal, age of onset of the disease and levels of transgene

expression. In different AD transgenic models, AHN was observed to be altered in both directions, decreased and increased (Winner and Winkler, 2015) (Lazarov et al., 2010) (Babcock et al., 2021).

3.1. AHN in 5xFAD mouse model

In 5xFAD mice, several studies confirm a decrease in the levels of neurogenesis that starts with the appearance of the first amyloid plaques. A significant reduction of immature DCX^+ GCs in the SGZ was seen compared to age-matched wild-type mice starting from 2 months of age (Moon et al., 2014)(Zaletel et al., 2018), or 3 months of age (Choi et al., 2018). This difference is almost abolished at 7 months of age, due to an age-dependent decrease in the number of neuroblasts in the WT animals (Moon et al., 2014). For what concerns cell proliferation in the SGZ, it was showed to not be altered in 2-months old 5xFAD mice (Zaletel et al., 2018), or to be instead significantly higher than controls (Choi et al., 2018). These results suggest that at early stages of the disease neurogenesis impairment is due to alterations in the process of differentiation or survival, rather than proliferation. Subsequently, even proliferation significantly decreases at 4- and 5- months of age, and the survival of proliferated cells is lower in 5xFAD than in WT as soon as 3 months of age (Choi et al., 2018). Contrasting results have been reported by Ziegler-Waldkirch et al. that demonstrate that in 4 months old 5xFAD mice, the number of both immature DCX^+ cells and proliferating $Ki67^+$ cells is significantly increased compared to healthy controls. At this age, the brain of the animal starts to show accumulation of Aβ peptides in hippocampal region. (Ziegler-Waldkirch et al., 2018).

Considering that development of AD has been reported to be more progressive in females 5xFAD than in males, gender differences have also been investigated. Unlike males, females of 2 months of age show a number of DCX^+ cells that is not significantly different between 5xFAD and healthy controls (Zaletel et al., 2018).

Additionally, significant impairment in pattern separation ability were observed in 5xFAD mice compared to age-matched WT mice starting at 5 months of age (Choi et al., 2018). Indeed, altering AHN has been shown to impact cognitive function. For example, genetic or pharmacological stimulation of neurogenesis accompanied with physical exercise or increased levels of brain derived neurotrophic factor (BDNF), significantly ameliorates cognitive deficits of the 6-months old animal and reduces amyloid burden (Choi et al., 2018).

3.2. AHN in AD patients

In humans, some studies indicate an age-related neurogenesis decline in healthy subjects, as reported before. One of these, found a statistically significant correlation between the density of DCX^+ cells and the age of the individual from 43 to 87 years of age (Moreno-Jimenez et al., 2019). The same group, examined a cohort of AD patients between 52 and 97 years of age, at different Braak stages. They consistently showed lower numbers of DCX^+ cells in tissues of affected individuals compared to neurologically healthy subjects. Interestingly, the decline in neurogenesis was observed even in patients at early Braak stages with still low levels of protein deposition (significant decrease starting from Braak Stage II). They demonstrated also that the density of neuroblasts correlates with the amount of tau tangles and Aβ plaques (Moreno-Jimenez et al., 2019). In a separate study, found a significant association between the number of proliferating neuroblasts (DCX^+ $PCNA^+$ cells) and cognitive ability was found, with a general trend of affected patients toward fewer DCX^+PCNA^+cells compared to healthy subjects. In this study, it was also observed a reduced neurogenesis in early stages of cognitive decline (Tobin et al., 2019). Both reported studies suggest a role of AHN in early stages of the disease, which may indicate AHN as integral part of AD pathology emergence.

Furthermore, even Zhou et al. analysing the transcriptome of hippocampal cells, observed a two-fold reduction of immature granule cells in AD patients' tissues compared to healthy controls. At the same time, the total percentage of granule cells remains constant between the two populations. They also implemented a cell–cell interaction analysis which revealed, in AD samples, a significantly decreased interactions of imGCs with other components of the niche, such as astrocytes, oligodendrocytes precursors cells, and GABAergic interneurons (Zhou et al., 2022).

Nevertheless, even in this case there are contrasting evidence to consider. Another study reported an increase in the expression of immature neuronal markers that has a tendency to rise accordingly with increase disease severity (Jin et al., 2004). However, the body of evidence that has been accumulated in more recent years, points towards an AD-related decline of both neuroblasts and newborn neurones.

An interesting finding in humans, to be confirmed by further investigations, is that individuals characterized by normal cognition, despite the presence of amyloid plaques and neurofibrillary tangles characteristic of a fully developed disease, have increased AHN compared to

patients with AD-related dementia (Briley at al., 2016). Hence the idea that adult born neurones, or neuroblasts themselves with their peculiar properties, could work as neuroadaptive response to preserve cognitive functions.

4. OXS-N1

OXS-N1 is a small molecule with proneurogenic abilities discovered through an *in vitro* phenotypic screening employing the neurosphere assay (NSA), by OxStem Neuro, a drug discovery company (Szele and Russell, unpublished data).

Due to the fact that mechanisms regulating neurogenesis are still to be clarified, a phenotype-based screening is a good approach to discover molecules that can increase neurogenesis, without a prior knowledge of a target pathway. In this project, the neurosphere assay was used to check the ability of small molecules to stimulate proliferation of neuronal progenitors, and differentiation into neurones. These neurosphere cultures were obtained from postnatal mouse neural stem cells derived from the SGZ and SVZ of C57Bl/6 mice of 3-6 days of age. The possibility to isolate and expand neuronal stem cells *in vitro* in serum-free culture system in presence of growth factors, was first demonstrated with cells of the SVZ of both developing and adult mouse brains (Reynolds and Weiss, 1992)(Reynolds and Weiss, 1996). The isolation of cells from postnatal brain, instead of adults, allows obtaining a higher amount of proliferating cells in culture with a consequent advantage of higher yields. This assay is design in order to select neural precursor cells by using EGF and/or FGF as growth factors since stem and progenitors cells are responsive to these mitogens that stimulate their active proliferation; whereas the majority of cells, namely differentiated cells, die in these culture conditions (Soares et al., 2020). Therefore, neural precursor cells can proliferate to form a ball of undifferentiated cells, the so-called neurosphere, which in turn can be dissociated to form more numerous secondary spheres, or be induced to differentiate, generating the three major cell types of the CNS: neurons, oligodendrocytes and astrocytes. Differentiation is stimulated by removing growth factors from the medium and using adherent culture conditions (Soares et al., 2020). With this system it was also possible to consistently demonstrate that cells isolated from niches of the mouse brain exhibit the stem cell attributes of proliferation, self-renewal, and the ability to give rise to a number of differentiated progeny (Reynolds and Weiss, 1992). Moreover, this assay is also useful to test drugs and

compounds to modulate NSCs properties since it is easy to manipulate the extrinsic cues the cells are exposed to during proliferation and/or differentiation phase, simply adding factors of interest to the media (Jensen and Parmar, 2006).

OXS-N1 resulted as the lead compound of the screening since it was the most capable to increase (1) proliferation of stem and progenitor cells and (2) differentiation of the aforementioned into neurones (Szele and Russell, unpublished data). In order to asses the first point, the number and diameters of neurospheres treated with the compound were measured; while for the second aspect, the ratio of neurones over astrocytes and oligodendrocytes was quantified after the induction of the monolayer of differentiated cells. Eventually, the molecule was tested *in vivo* in order to define its pharmacokinetics properties, and it has been proven to cross the BBB.

In a subsequent study, the mechanism of action of the molecule was investigated in order to proceed with a hit-to-lead optimisation of the compound, and to have an insight in the molecular pathways that may regulate neurogenesis (Szele and Russell, unpublished data). To uncover the target of OXS-N1, an affinity-based protein profiling was employed in NSA in SVZ- and DG-derived murine neural stem cells. In this system, the molecule was developed into a chemical probe bearing a photo affinity label that after exposure to UV light crosslinks with the cellular targets, and an alkyne tag that following cell lysis and after being subjected to a click reaction, binds to biotin for affinity enrichment. The enriched conjugated proteins obtained with this probe, were then analyzed by mass spectrometry and after subsequent target validation, vimentin was revealed as target of OXS-N1. Vimentin is a cytoskeletal protein, specifically an intermediate filament (IF) type III, that is expressed by neural progenitors and in astrocytes, together with GFAP and nestin (Seri et al., 2001).

Aim of the project

The main goal of this project is to asses the ability of OXS-N1 to increase neurogenesis *in vivo,* particularly in the subgranular zone, and thereby improve the performance of animal models in memory tasks, especially the ones involving pattern separation.

This work takes into consideration two *in vivo* studies based on a wild-type (WT) mouse model, C57Bl/6, and an animal model of familial Alzheimer's disease, the 5xFAD mouse. This transgenic model has been crossbred with the MacGreen mouse model (genetic background: C57Bl/6) expressing EGFP under the control of the mouse colony stimulating factor 1 receptor (*Csf1r)* promoter. The transgene mimics the endogenous gene expression and labels the myeloid cell lineage, in particular in CNS microglia and brain infiltrating macrophages (Sasmono et al., 2002).

5xFAD mice, 19-24 weeks old, were divided into two groups: half of them, 14 mice, were treated with the putative neurogenic small molecule OXS-N1, while the other half, 13 mice, was administered with vehicle. The treatment comprises 1 week of oral administration by pipette of 25mg/kg OXS-N1, 3 times per day. The same week of the OXS-N1 treatment, 1mg/ml of BrdU was added in drinking water. The same protocol was followed in a separate study, in which the compound or the vehicle were administered to a cohort of 32 thirteen-weeks-old wild type C57 Black 6 mice. After one week of wash-out after drug administration, the behavioural analysis was performed.

The behavioural analysis was carried out at the Winter Lab at Humboldt University, using a fully automated touchscreen test battery. The advantage of this experimental setting is that mice can individually enter the touchscreen chamber 24/7 in a self-motivated fashion whilst being grouped-house in their home cage. This allows for minimal experimenter intervention, that can greatly influence the outcome of behavioural tests (Richter et al., 2020). In the test chamber, the animals perform cognitive tasks on a touchscreen and get nutritional pellets as rewards without the need for prior food deprivation. Two tasks were used to assess cognitive and executive functions in mice, with a main focus on functions that are related to adult hippocampal neurogenesis such as pattern separation. In the location discrimination (LD) task, the animals' pattern separation ability is tested by the need to differentiate between different stimulus locations with varying distances on the touchscreen. The task also tests cognitive flexibility by including reversals of the correct stimulus location. Task performance in the LD task was evaluated to be sensitive to changes in adult

hippocampal neurogenesis. In the Paired-Associated Learning (PAL) task, the animals learn to associate an object/image with its designated correct location on the touchscreen. The task thus tests associative memory and was evaluated as sensitive to hippocampal dysfunction. After 2 weeks of pre-training for touchscreen experiments, behavioural analysis were performed for 7 weeks in the case of 5xFAD mice, and 13 weeks in the case of WT mice. The time difference was due to issues with learning and performance speed of WT mice, possibly linked to unexpected teeth and weight problems, that led to an overall prolonged experiment time in order to achieve a certain amount of sessions to analyse. The behavioural testing overall revealed no significant differences between the vehicle and the OXS-N1 treated animals neither in WT nor in 5xFAD mice.

The aim of my project is to perform an histological analysis on the brains of mice used in the aforementioned studies, in order to investigate the process of adult hippocampal neurogenesis. In this way it is possible to assess the *in vivo* pro-neurogenic abilities of the small molecule OXS-N1.

Materials and Methods

At Winter Lab in Humboldt University, following behavioural tests mice were sacrificed by intraperitoneal injection of pentobarbital and perfused with 4% paraformaldehyde (PFA). Brains were removed and fixed with 4% PFA overnight at 4oC before being transferred to 30% sucrose in PBS for 48h at 4°C.

Sample preparation and Immunohistochemistry. Coronal brain sections, 30μm thick, were obtained from fixed and frozen brains using the sliding microtome (Leica SM2000R) and dry ice. Sections were stored at −20°C in cryoprotectant solution (ethylene glycol, sucrose, 0.1M phosphate buffer composed of 0.2M NaH_2PO_4 and 0.2M Na_2HPO_4 in distilled water) until usage. For immunolabeling, we considered 3 dorsal hippocampal sections and 3 sections that include lateral ventricles per mouse; in stereotaxic coordinates for the mouse brain, we picked sections from Bregma -1.5mm to -2.5mm to analyse the SGZ, and from Bregma 0.5mm to 0mm for SVZ. All sections were transferred to a fresh well with Phosphate Buffered Saline (PBS) and washed in PBS 5 x 7 minutes to remove excess cryoprotectant solution. Single, double or triple immunohistochemistry was then performed; only for the purpose of staining antigens that require antigen retrieval (BrdU), sections were incubated for 1h at 37°C in 1ml of hydrochloric acid (HCl, 1M). After this step, all sections were incubated with 50mM glycine in PBS for 15 min to reduce autofluorescence of PFA-fixed tissue. Sections were washed in PBS 3 x 5 min before blocking for 1h at RT in blocking buffer (PBS containing 0.5% Triton X-100 (PBS-T) and 10% Donkey Serum). Sections were then incubated overnight under gentile shaking at 4°C with primary antibody diluted in blocking buffer while secondary antibody controls were kept in blocking buffer. The next day, sections were washed in PBS-T 3 x 5 min and then they were incubated with fluorochrome-conjugated secondary antibody diluted in blocking buffer at RT in the dark for 1 hour under gentile shaking. Sections were washed in PBS-T 3 x 5 min before staining with DAPI (1:1000 in PBS) for 2 minutes at RT. After a single PBS rinse, sections were mounted onto a glass slide and allowed to dry before FluorSave was applied and the slides covered. Sections were allowed to dry for 1 hour and then sealed and kept at 4°C until imaging. All the steps after incubation with secondary antibody were performed in the dark.

Primary antibodies used were: Goat anti-Iba1 (1:300, Abcam ab5076), Rabbit anti-CD68 (1:2000, Abcam ab125212), Mouse anti-β-Amyloid (1:500, monoclonal IgG1, κ; clone 6E10; BioLegend SIG-39320), Mouse anti-doublecortin (1:400, DCX; CST4604S), Mouse anti-NeuN

(1:300, MAB377), Sheep anti-BrdU (1:200, ab1893), Rabbit anti-GFAP (1:200 Sigma- Aldrich, G9269).

Alexa Fluor–coupled fluorescent secondary antibodies (Thermo Fisher) were used at dilution 1:1000: Donkey Alexa-488 anti-rabbit (A21206), Donkey Alexa-568 anti-goat (A11057), Donkey Alexa-568 anti-rabbit (A10042), Donkey Alexa-647 anti-mouse (A31571), Goat Alexa-488 anti-mouse (A28175), Donkey Alexa-568 anti-sheep (A-21099), Goat Alexa-647 anti-rabbit (A27040).

Image acquisition. For evaluation of results, epifluorescent images were obtained using a Nikon Eclipse-Ti microscope (Nikon) and Volocity software. We acquired single-plane images at 10X magnification that include the whole granule cell layer, or 10X tile scans to visualise the entire perimeter of lateral ventricles, or Z-stacks at 2μm spacing at 40X magnification employed for the quantification of positive cells. In order to perform a qualitative morphological analysis, and obtain representative images at higher magnification (63X), Z-stacks were acquired with the Zeiss LSM 710 laser scanning confocal microscope.

Stereological cell count. Stereological methods were used for cell counting and to estimate the number of positive cells for each specific marker. All quantifications were done by an observer blinded to experimental condition. Quantification was done using FIJI (ImageJ) software. For DCX^+ cells' counting, the whole GCL was considered: its area was measured on 10X images on the DAPI channel using the free hand tool on ImageJ, then multiplied for the thickness of the section (30μm) to derive the volume. DCX^+ cells inside the reference volume were counted on individual planes considering 40X Z-stacks, then the number was divided by the volume to obtain cell density (number of cells/mm^3). To perform a subregional analysis we divided the counted cells depending on their location in suprapyramidal, infrapyramidal blades or crest, and the area of each region was measured as described before. For counting of $BrdU^+$ cells, co-labelled with NeuN or GFAP, the same process was followed. For the purpose of analysing and comparing the morphology of DCX^+ cells, 10 confocal Z-stacks per group were considered, at max-intensity projection. For microglia cells' counting, one representative image at 40X magnification was considered for each section: microglia cells in the whole image were counted on individual planes, and the total area of the image was considered to derive the cell density. Finally, in order to qualitatively assess the number and localisation of DCX^+ cells in the SVZ, 10X tile scans were considered.

Statistical analysis. Statistical analysis was performed using GraphPad Prism software. The D'Agostino and Pearson test was used to check the normality of sample distribution for $n>5$, while the Shapiro-Wilk test was used for experiments with $n\leq5$. For comparisons between two experimental groups, unpaired two-tailed Student's t-test with 95% confidence interval was used in the case of normal sample distribution, which was always the case. Results were considered statistically significant when $p < 0.05$. Graphs represent mean values ± s.e.m.

Results

1. 5xFAD mice

We focused our studies on the dorsal DG as this anatomical region is associated with spatial learning and memory functions, whereas the ventral hippocampus is related to stress response and emotional behaviour (Fanselow and Dong, 2010).

In order to have a qualitative idea of the magnitude of the damage to the brain of 5xFAD mice, aged 31-37 weeks at the time of perfusion, we stained the tissue for Aβ and observed the extent of amyloid plaques deposition. In addition, we stained microglia for CD68 which is a lysosomal-associated membrane protein expressed at high levels by macrophages and activated microglia and at low levels by resting microglia, that could play a role in phagocytic activities (Hopperton et al., 2018). CD68 is specifically up-regulated in disease-associated microglia (DAM) subtype which is found in proximity to Aβ plaques (Keren-Shaul et al., 2017).

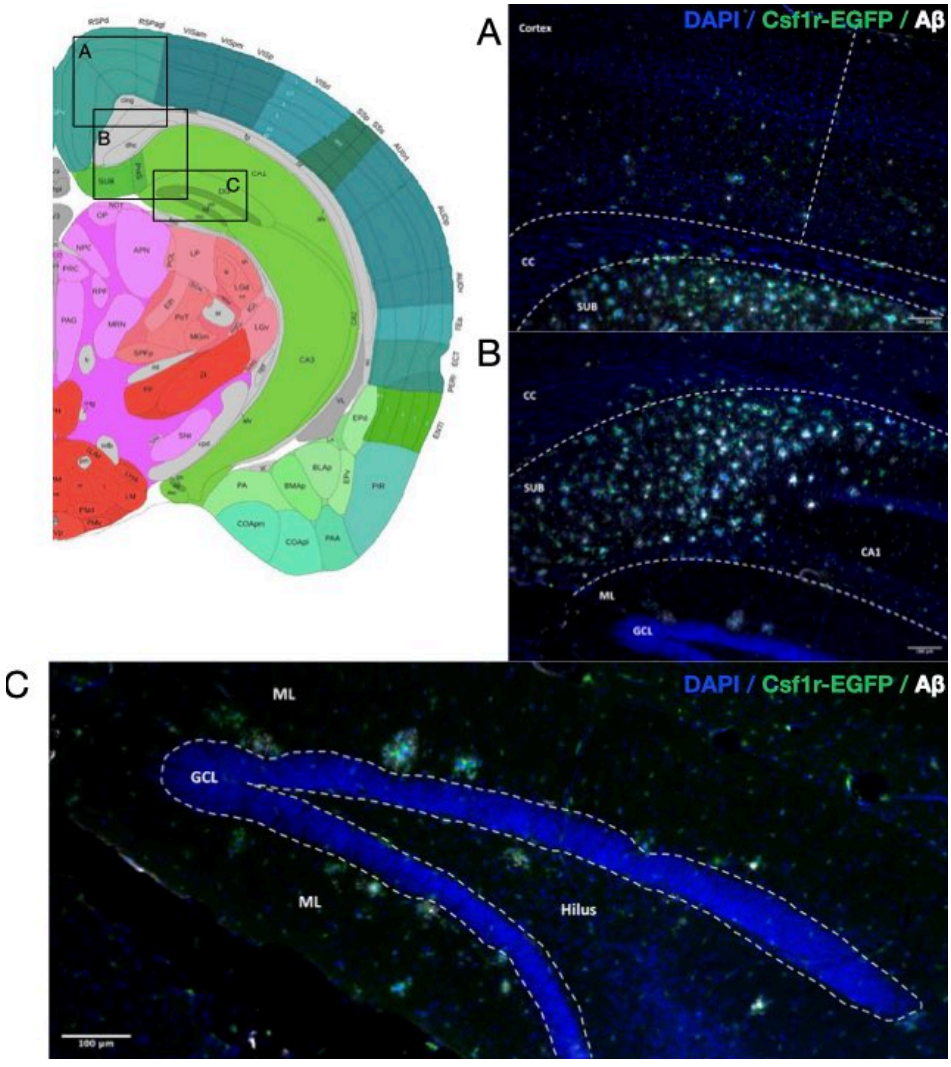

Figure 1. Representative images of cortex (A), subiculum (B) and dentate gyrus (C) of a 5xFAD mouse brain section, showing amyloid β deposits (white) and microglia cells (green). CC = Corpus Callosum, SUB = Subiculum, ML = Molecular Layer, GCL = Granule Cell Layer, CA1 = Cornu Ammonis 1.

We observed a high density of plaques and microglia cells in the subiculum (Fig.1A), which is one of the first regions affected by the proteic deposits in 5xFAD mice (Oakley et al. 2006). Aβ plaques are observed also in the cortex, mainly the deeper layers (Fig.1B), indeed pyramidal neurons of layer 5 are the first to be lost (Oakley et al. 2006). For what concerns the dentate gyrus, several plaques disrupting the integrity of the granule cell layer (GCL) are visible, always surrounded by microglia cells (Fig.1C). We observed toxic accumulations in molecular layer (ML) and hilus as well. (Fig.1C) We further investigated the appearance of Aβ plaques at high magnification (Fig.2): we can see activated microglia cells extending their processes towards the amyloid β accumulation.

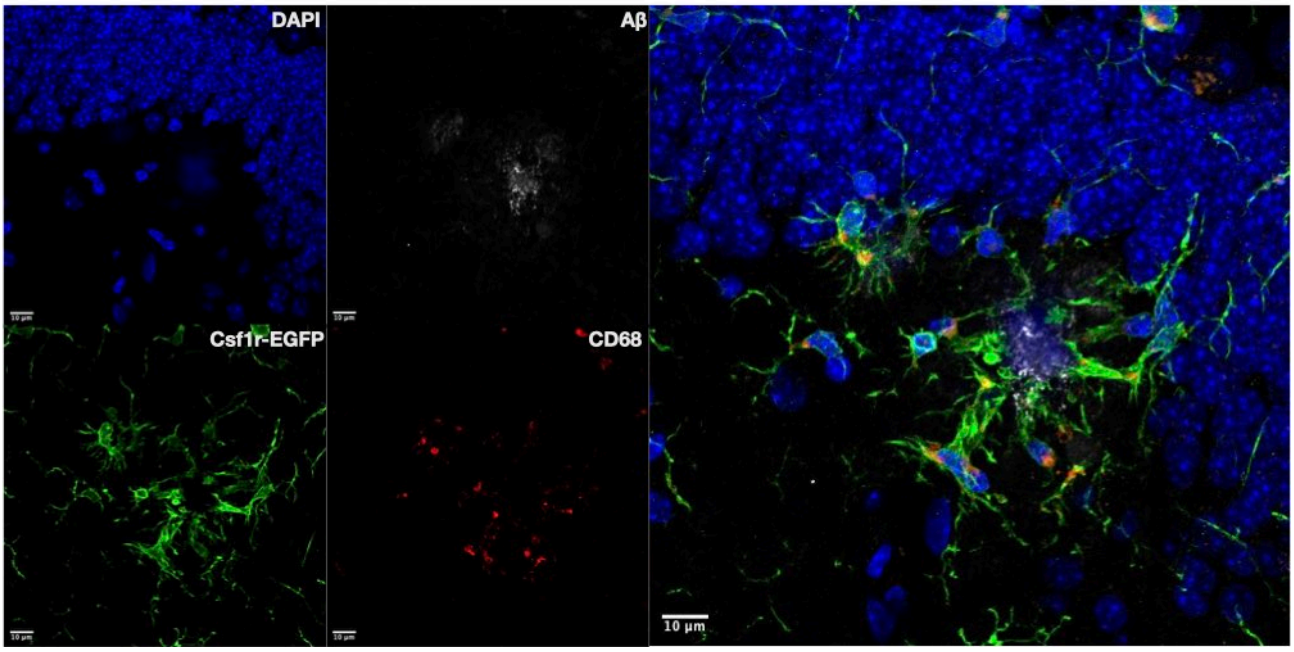

Figure 2. Detail of an Aβ plaque (white) surrounded by microglia cells (green), disrupting the GCL of a 5xFAD mouse. Microglia cells co-label with a protein indicative of their activation, CD68 (red).

To assess a possible effect of OXS-N1 on the extent of neurogenesis in treated mice, we stereologically counted the number of DCX^+ immature neurons (Fig.3A) in the DG of both populations, vehicle and drug administered animals (n = 13 vehicle, n = 14 OXS-N1). We did not observe any significant difference in the density of DCX^+ cells (cells/mm3) between vehicle and OXS-N1 treated 5xFAD mice (Fig.3B, $p = 0.71$). Given the differences between the blades of the granule cell layer, we then considered these different regions and separated the labelled cells according to their location, (Fig.3C.; suprapyramidal blade, infrapyramidal blade and crest) and determined the density of DCX^+ cells in each specific volume. We did not observe any significant difference in the density of labelled cells between vehicle and OXS-N1 treated mice in any of the DG subregions (Fig.3D). Due to differences observed in the extent of neurogenesis between male

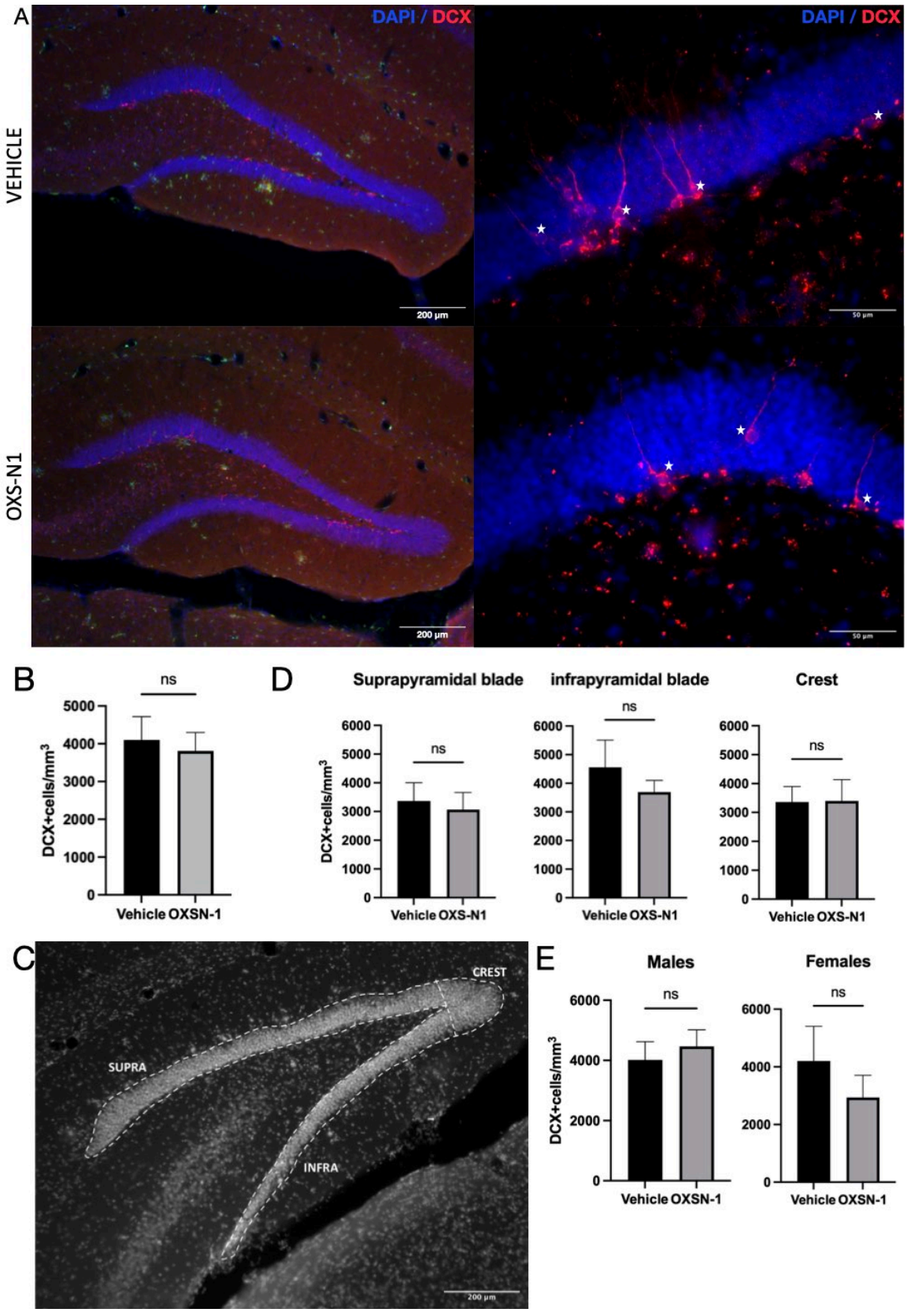

Figure 3. DCX+ cells (red) in 5xFAD mice. (A) Representative images of the staining for doublecortin: entire DG and infrapyramidal blade at higher magnification, in vehicle (upper images) and OXS-N1 treated mice (lower images). White stars indicate examples of DCX+ cells. (B) Quantification and analysis of DCX+ cell density: n=13 vehicle, n=14 OXS-N1. Two-tailed T-test: p = 0.71. (C) Representative image of the DG in DAPI channel. SUPRA = supra pyramidal blade, INFRA = infra pyramidal blade, CREST = crest. (D) Subregional quantification and analysis of DCX+ cell density: n=13 vehicle, n=14 OXS-N1. Two-tailed T-test: supra p = 0.74, infra p = 0.97, crest p = 0.42. (E) Analysis of DCX+ cell density divided by gender. Two-tailed T-test. Males: n=7 vehicle, n=8 OXS-N1, p = 0.59. Females: n=6 vehicle, n=6 OXS-N1, p = 0.40.

and female 5xFAD mice, as well as gender differences are known to exist in the progress of the AD pathology, we performed a separate analysis for male and female mice and also in this case we did not observed any difference (Fig.3E).

We then asked if OXS-N1 could promote the maturation of neuroblasts, hence their integration into the hippocampal circuit, rather than increasing the production of new neurones. For this purpose we considered the dendrites of DCX^+ cells extending into the molecular layer, and observed length and dendritic branching, as well as location of these neuroblasts in the GCL or in SGZ (Fig.4). Even in this aspect we did not observed visible differences between OXS-N1 treated and vehicle administered mice, which could justify a quantitative analysis of these parameters.

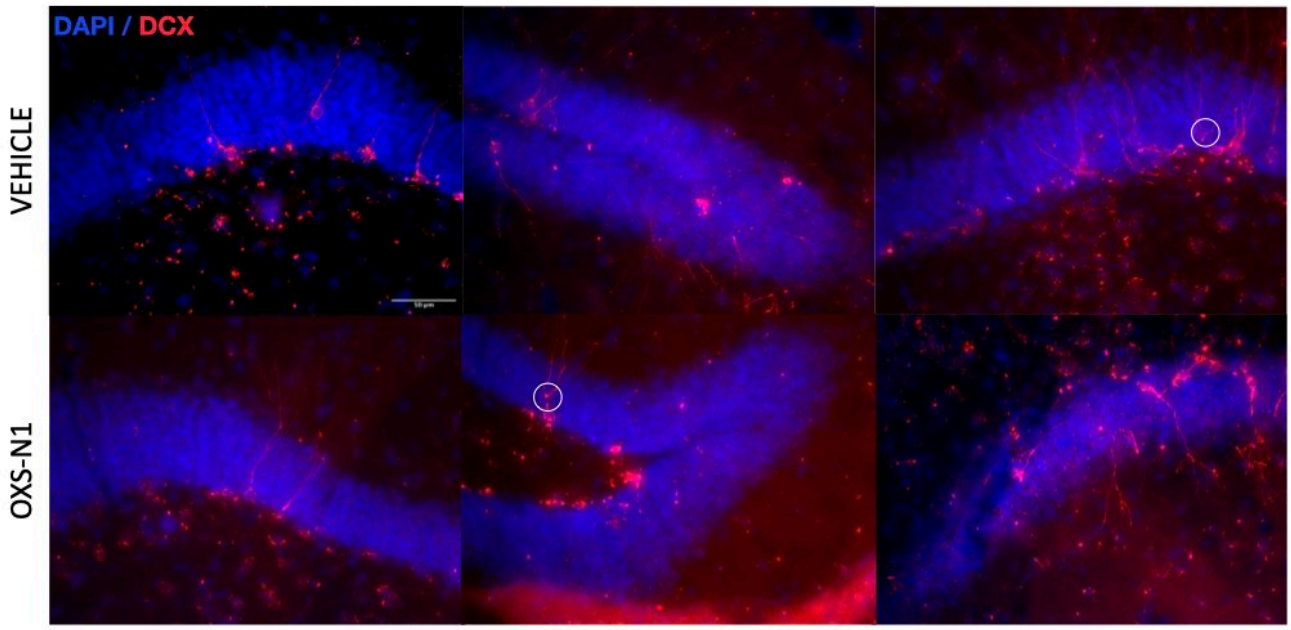

Figure 4. Representative confocal images of suprapyramidal blade, infrapyramidal blade and crest of vehicle administered mice (upper images) and OXS-N1 treated mice (lower images). Max intensity projections of confocal z-stacks at 1 µm spacing. White circles indicate examples of branching dendrites in GCL observed in both animal populations.

Next, in order to quantify the extent of proliferation, we detected the BrdU present in the tissue, and we co-labelled $BrdU^+$ cells with NeuN, a marker of mature neurons (Fig.5A,B n = 13); the double-labelled cells were considered mature neurons that were born during the time of BrdU administration. We stereologically counted the $BrdU^+NeuN^+$ cells and did not observe any significant differences in their density in 5xFAD mice treated with vehicle or OXS-N1 (Fig.5C, $p = 0.12$). Surprisingly, the regional analysis, as performed before, showed a decrease in the density of double-labelled cells in the infrapyramidal blade of the DG of mice administered with the drug (Fig. 5D, $p = 0.0319$). This was not observed for the other two subregions of the DG (Fig.5D).

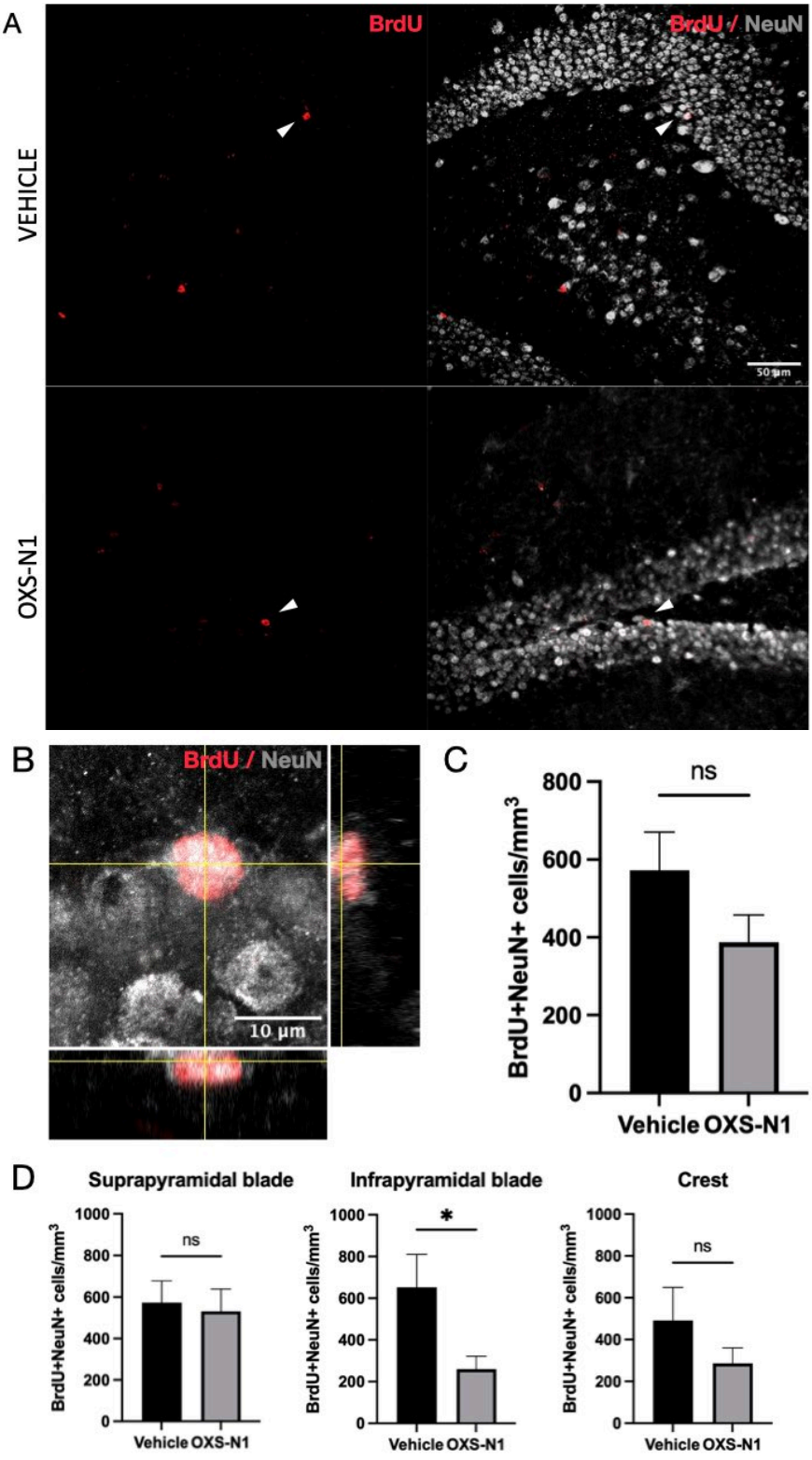

Figure 5. BrdU⁺NeuN⁺ cells in 5xFAD mice. (A) Representative confocal images of double positive cells for BrdU (red) and NeuN (grey), in vehicle (upper images) and OXS-N1 (lower images) treated mice. (B) High magnification of a double positive cells with orthogonal projection. (C) Quantification and analysis of BrdU⁺NeuN⁺ cell density: n = 13 vehicle, n = 13 OXS-N1. Two-tailed T-test: p = 0.12. (D) Subregional quantification and analysis of BrdU⁺NeuN⁺ cell density: n = 13 vehicle, n = 13 OXS-N1. Two-tailed T-test: supra p = 0.78, infra p = 0.03, crest p = 0.26.

To determine whether OXS-N1 affects proliferation specifically of neural stem cells, we co-labelled BrdU$^+$ cells with glial fibrillary acidic protein (GFAP) in a subset of the animals (n = 3) to identify the dividing neural stem cell population (Fig.6A,B). We counted the BrdU$^+$GFAP$^+$ cells as before, and we did not observe significant differences between vehicle and OXS-N1 treated animals (Fig.6C). Separating the cells according to their subregional localization also did not reveal any significant differences (Fig.6D).

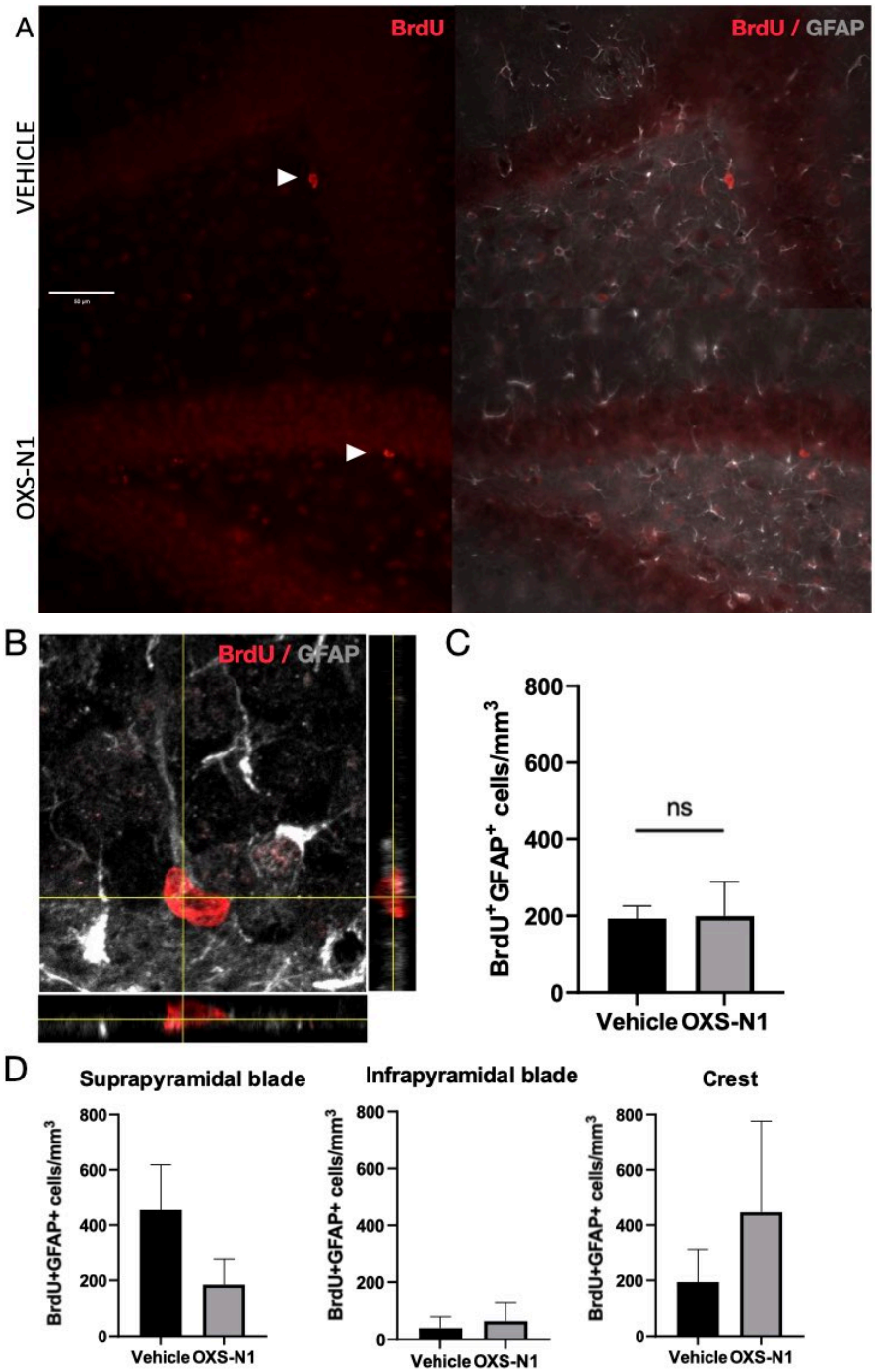

Figure 6. BrdU$^+$GFAP$^+$ cells in 5xFAD mice. (A) Representative images of double positive cells for BrdU (red) and GFAP (grey), in vehicle (upper images) and OXS-N1 (lower images) treated mice. (B) High magnification of a double positive cells with orthogonal projection. (C) Quantification and analysis of BrdU$^+$GFAP$^+$ cell density. n = 3, two-tailed T-test: p = 0.22. (D) Subregional quantification and analysis of BrdU$^+$GFAP$^+$ cell density. n = 3 vehicle, two-tailed T-test: supra p = 0.14, infra p = 0.95, crest p = 0.95.

We then asked if OXS-N1 could be affecting AHN indirectly though the modulation of neuroinflammation. It is not known if activated microglia in SGZ is detrimental or beneficial for neurogenesis. However, there are some evidences that see microglia modulating the process of adult hippocampal neurogenesis, specifically phagocyting apoptotic newborn cells in SGZ (Sierra et al. 2010). Accordingly, we quantified the density of Csf1r-EGFP^{+} microglia cells in the hippocampal region in a subset of the animals (n = 3), in order to use the density of microglia as indicator of inflammation levels in the brain region. We did not find a significant difference. (Fig.7A,B)

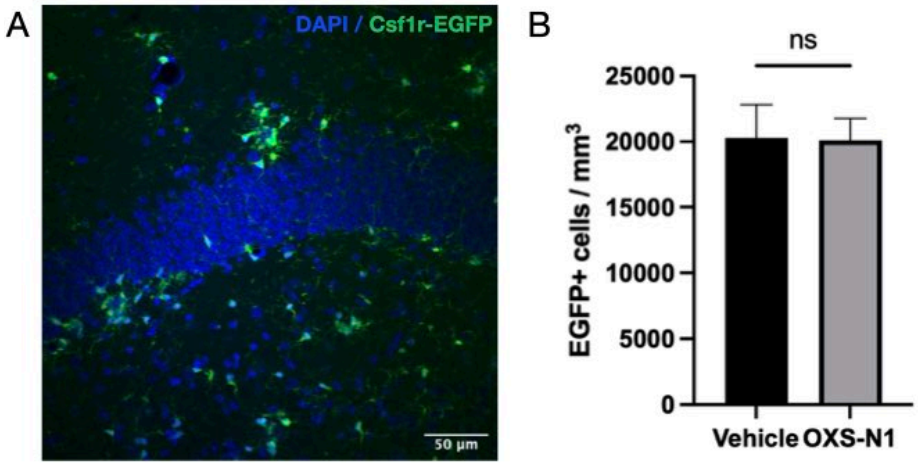

Figure 7. Microglia cells in 5xFAD mice. (A) Representative confocal image of the dentate gyrus with microglia cells (green). (BI Quantification and analysis of microglia cell density. n = 3, two-tailed T-test: p = 0.95.

In order to assess if OXS-N1 could be affecting the other neurogenic niche in the brain, we stained for doublecortin more anterior sections of the brain for a subset of the animals (n = 3), so as to observe the SVZ. We qualitatively analyze the presence and localizations of neuroblasts (Fig. 8A,B) and even in this case, no differences between the two groups were observed.

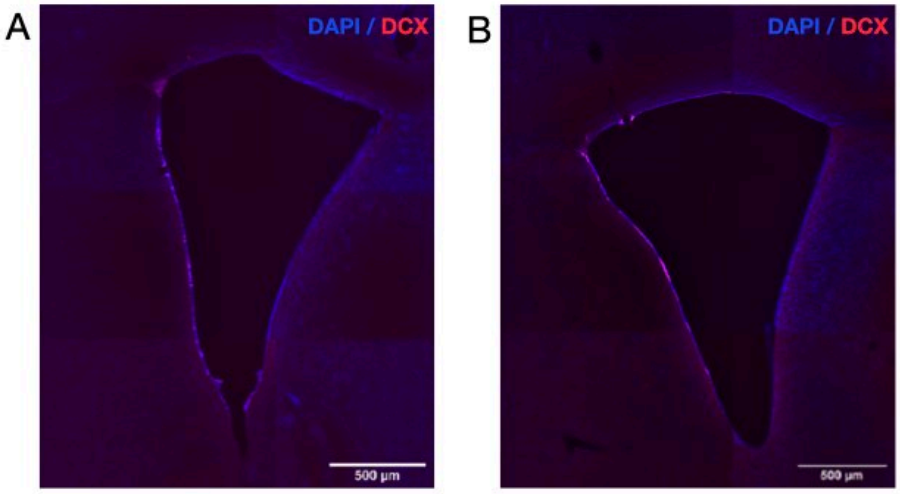

Figure 8. Representative tile scans of SVZ in 5xFAD mice. Staining: doublecortin (red) and nuclei (blue). (A) Vehicle treated mouse. (B) OXS-N1 treated mouse.

2. C57Bl/6 mice

To determine the effect of OXS-N1 on neurogenesis in wild type C57Bl/6 mice, we performed a similar histological analysis. These animals were 29 weeks old at the time of perfusion.

We measured the density of DCX^+ immature neurones of the DG as done before (Fig. 9A; n = 16), which did not show any significant difference between vehicle and OXS-N1 treated mice (Fig. 9B, p = 0.66). It is noteworthy that the amount of DCX^+ cells in wild type animals is much more abundant, both visually and looking at the data, compared to 5xFAD mice; these studies however are not comparable since have been performed separately and for a different time period, additionally the age of the WT and 5xFAD populations at the time of the experiments is different as well. The subregional analysis based on the location of $doublecortin^+$ cells in the DG, did not result in significant difference between the density of labelled cells (Fig.9C). Given the fact that neurogenesis levels in 5xFAD have been showed to vary during aging depending on the gender, we performed a separate analysis for males and females and even in this case there are not significant differences (Fig.9D). We observed only a statistically significant difference between wild type males and females, in both cases where they were administered with OXS-N1 or vehicle (data not shown), that confirm a decline in AHN that differs between genders, but that is not indicative of the drug's activity.

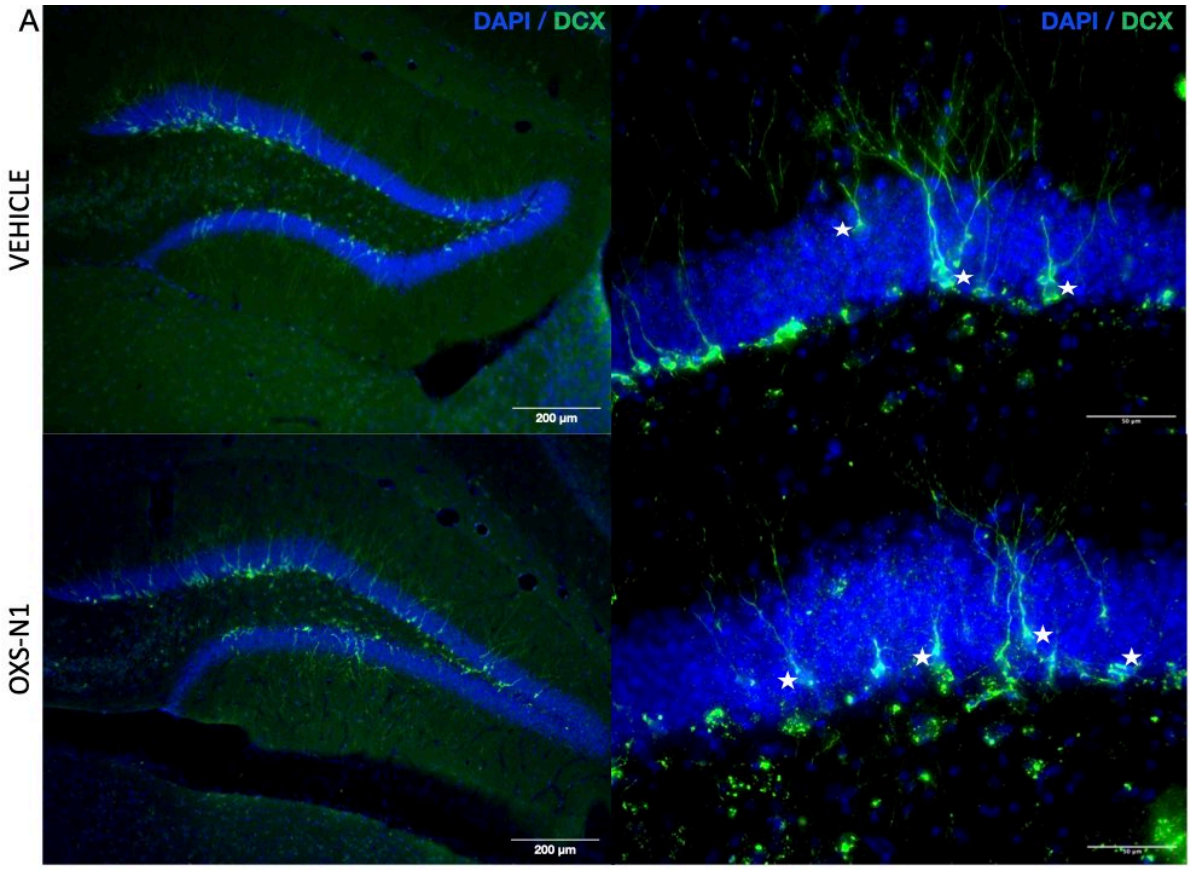

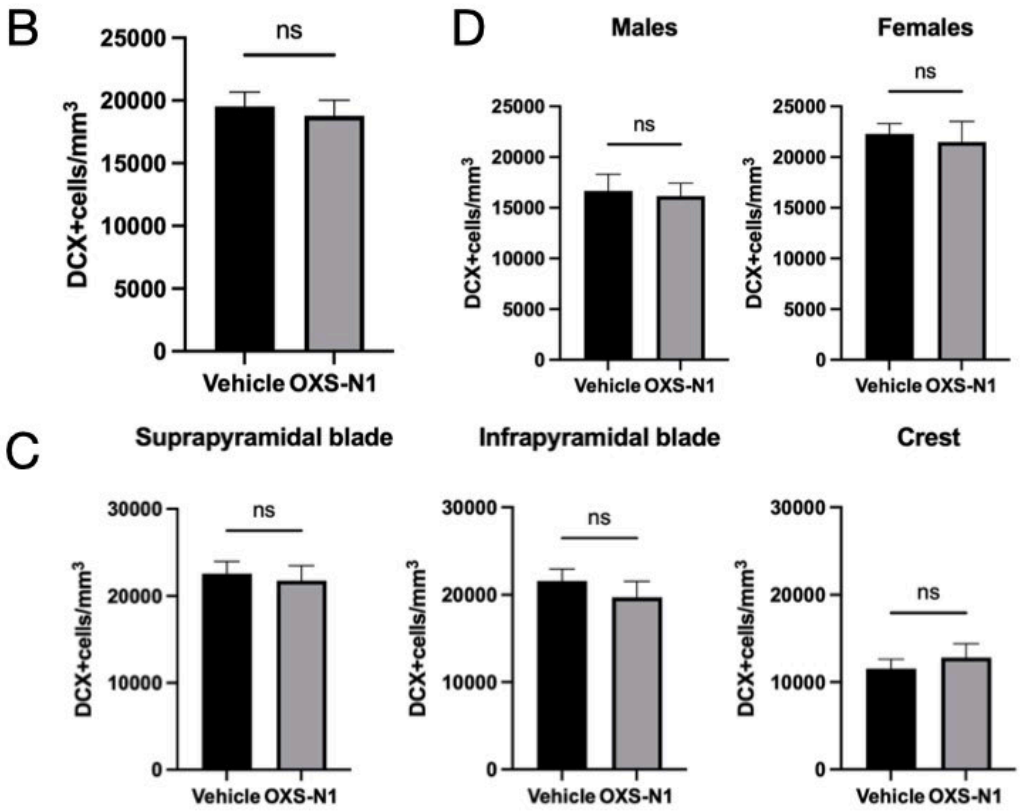

Figure 9. DCX+ cells (green) in C57Bl6 mice. (A) Representative images of the staining for doublecortin: entire DG and infrapyramidal blade at higher magnification, in vehicle (upper images) and OXS-N1 treated mice (lower images). (B) Quantification and analysis of DCX+ cell density. n = 16, two-tailed T-test, p = 0.66. (C) Subregional quantification and analysis of DCX+ cell density. n = 16, two-tailed T-test, supra p = 0.72, infra p = 0.41, crest p = 0.72. (D) Analysis of DCX+ cell density divided by gender. Two-tailed T-test. Males: n=7 vehicle, n=8 OXS-N1, p = 0.82. Females: n=7 vehicle, n=7 OXS-N1, p = 0.73.

Additionally, a possible impact of OXS-N1 on maturation of neuroblasts was evaluated. Visually, the dendritic length and branching of DCX+ cells extending into the molecular layer, did not show any difference comparing OXS-N1 treated and vehicle administered mice. (Fig.10) Therefore, as considered before, we did not proceed with the measurement of these parameters.

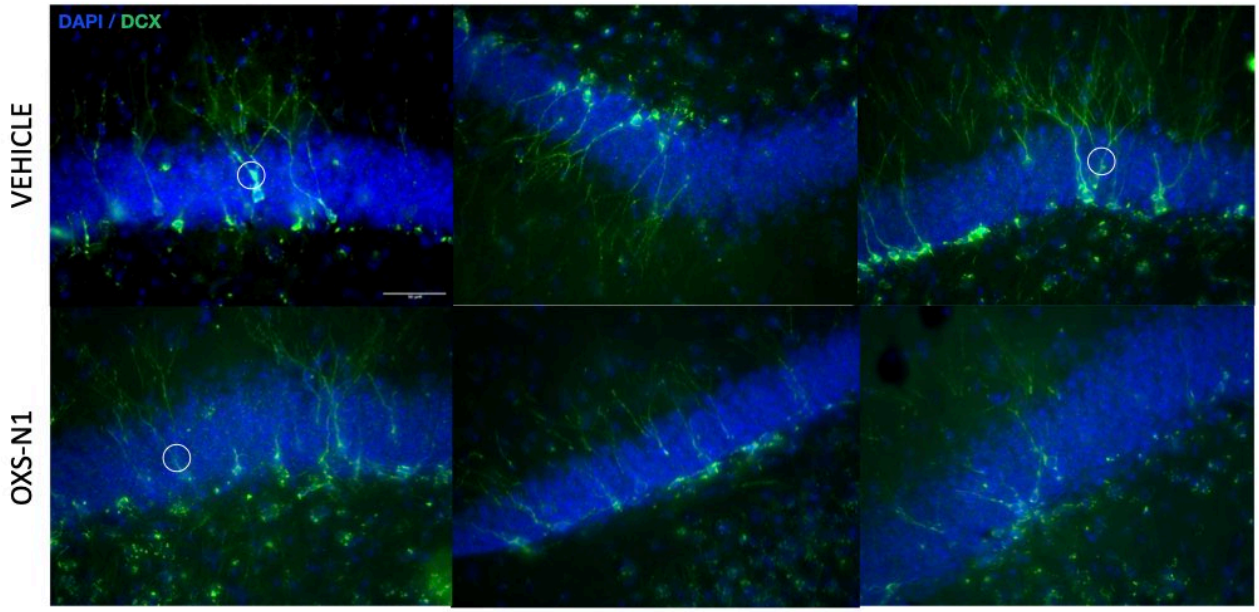

Figure 10. Representative confocal images of suprapyramidal blade, infrapyramidal blade and crest of vehicle administered mice (upper images) and OXS-N1 treated mice (lower images). Max intensity projections of confocal z-stacks at 1 µm spacing. White circles indicate examples of branching dendrites in GCL observed in both animal populations.

In order to assess the effect of OXS-N1 on the levels of mature neurons that were born during the time of BrdU administration, we co-labelled BrdU+ cells with NeuN (Fig.11A, n = 16). The comparison of the density of $BdU^{+}NeuN^{+}$ cells did not reveal any significant difference in C57Bl/6 mice treated with OXS-N1 in comparison to mice administered with vehicle (Fig. 11B $p = 0.11$). Separating the cells into subregions did not result in statistically significant results (Fig.11C). Although in the infrapyramidal blade there is a trend towards a higher density of double positive cells in vehicle-administered mice ($p = 0.06$), which seems to confirm the same finding observed in 5xFAD mice. As observed for DCX^{+} cells, also the density of $BrdU^{+}NeuN^{+}$ cells appeared higher in C57Bl/6 mice than in the 5xFAD mice.

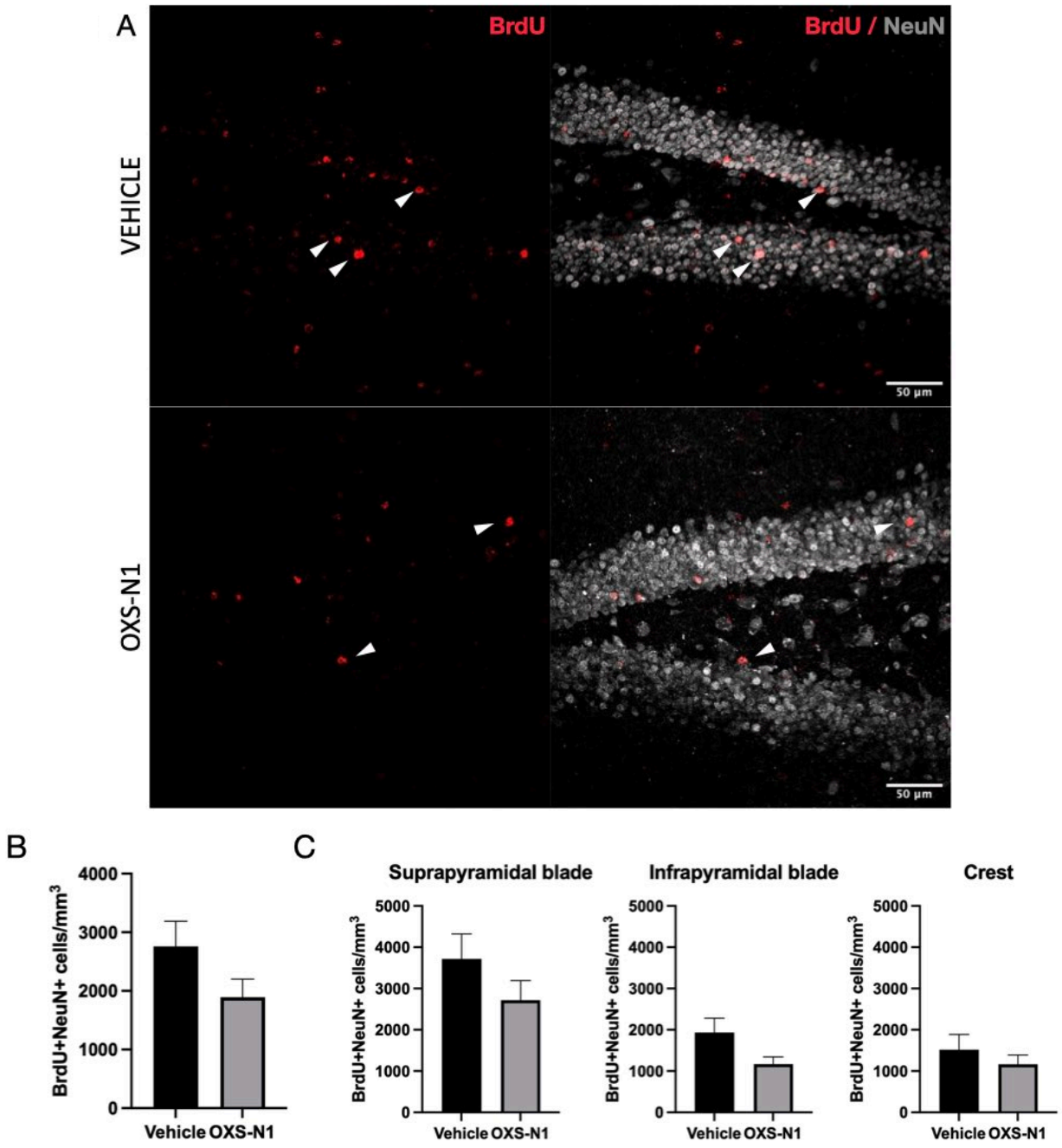

Figure 11. BrdU⁺NeuN⁺ cells in C57Bl/6 mice. (A) Representative confocal images of double positive cells for BrdU (red) and NeuN (grey), in vehicle (upper images) and OXS-N1 (lower images) treated mice. (B) Quantification and analysis of BrdU⁺NeuN⁺ cell density. n = 16, two-tailed T-test, p = 0.11. (D) Subregional quantification and analysis of BrdU⁺NeuN⁺ cell density. n = 16, two-tailed T-test: supra p = 0.2, infra p = 0.06, crest p = 0.42.

We then measured the density of cells co-labelled with BrdU and GFAP in a subset of the C57Bl/6 population (n = 3), to evaluate the impact of OXS-N1 on neural stem cell proliferation. Once again, the stereological counting of these double labelled cells did not reveal significant differences between vehicle and OXS-N1 treated animals (Fig.12). The analysis divided for supra-, infra-blades and crest did not reveal any statistical difference.

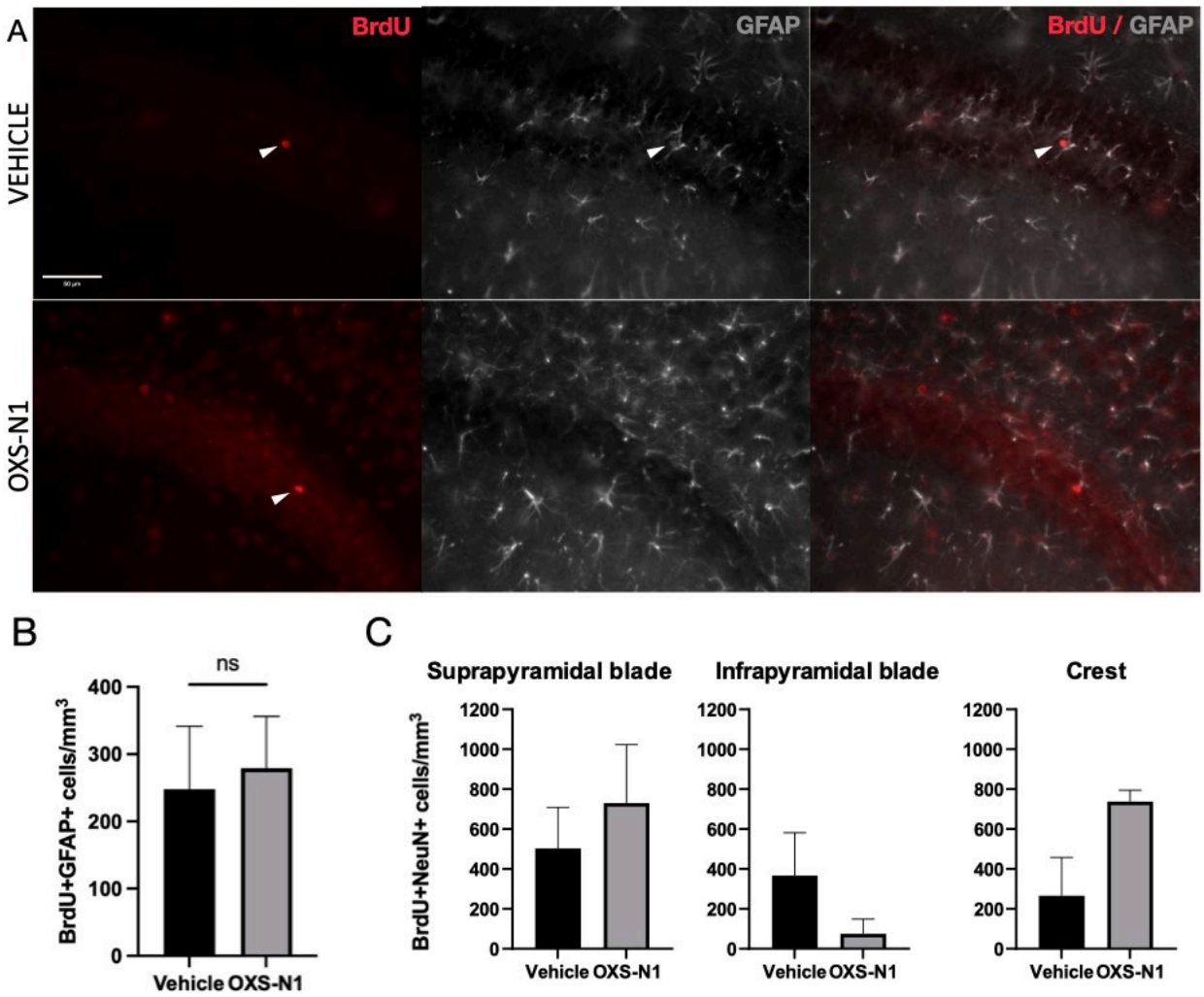

Figure 12. BrdU+GFAP+ cells in 5xFAD mice. (A) Representative images of double positive cells for BrdU (red) and GFAP (grey), in vehicle (upper images) and OXS-N1 (lower images) treated mice. (B) High magnification of a double positive cells with orthogonal projection. (C) Quantification and analysis of BrdU+GFAP+ cell density. n = 3, two-tailed T-test: p = 0.81. (D) Subregional quantification and analysis of BrdU+GFAP+ cell density. n = 3 vehicle, two-tailed T-test: supra p = 0.71, infra p = 0.27, crest p = 0.19.

To determine the effect of OXS-N1 on neuroinflammation in C57Bl/6 mice, we analysed a subset of the animals (n = 3) for Iba1 immunoreactivity (Fig.13A). We quantified the density of Iba1+ microglia in the hippocampal region and did not find a significant difference between vehicle and OXS-N1 treated animals (Fig.13B). To be sure that the antigen and the antibody used were giving the same information as the expression of GFP under the *Csf1r* promoter in 5xFAD-

MacGreen mice, we stained some brain sections of 5xFAD for Iba1 following exactly the same protocol, and assessed the colocalization of the two fluorescent signals. It is interesting to note that in wild type animals' tissue, the microglia population looks more homogeneously distributed and not clumped into clusters as it was in 5xFAD mice tissues. Indeed these cells in wild type mice present long, ramified processes with small cell bodies which are typical morphological characteristics of resting ramified microglia, whereas in 5xFAD it is possible to observe cells with enlarged cell bodies and fewer and swollen processes which are features associated with pro-inflammatory activation of these so-called ameboid microglia cells (Cunningham et al., 2013).

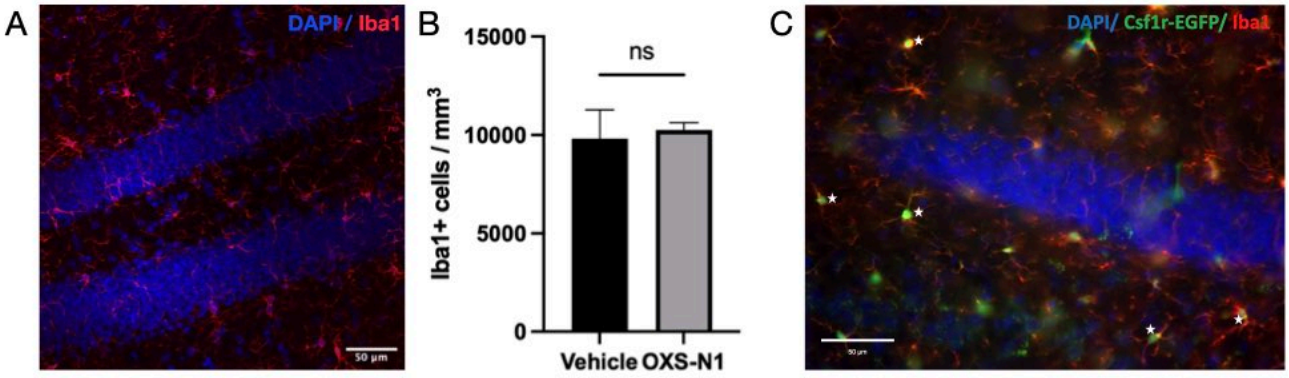

Figure 13. Microglia cells in C57Bl6 mice. (A) Representative confocal image of the dentate gyrus with microglia cells (red). (Bl Quantification and analysis of microglia cell density. n = 3, two-tailed T-test: p = 0.8. (C) Image showing the co-localization of Csf1r-EGFP (green) and Iba1 (red) expression in 5xFAD mouse brain section. White star indicate examples of double positive cells.

To determine if OXS-N1 was affecting neurogenesis in the other neurogenic niche, we compared DCX-immunoreactivity in a subset of the animals (n = 3) specifically in SVZ. Once again, we did not observe a qualitative difference between the vehicle and OXS-N1 treated animals (Fig.14). Similar to the DG, we visually observed more DCX-immunoreactive cells in the SVZ of C57Bl/6 animals than in 5xFAD. Additionally, we it was possible to see clearly the difference in the anatomy of the lateral ventricles between WT and 5xFAD mice, with the latter having enlarged ventricles due to global cerebral atrophy (Leung et al., 2013).

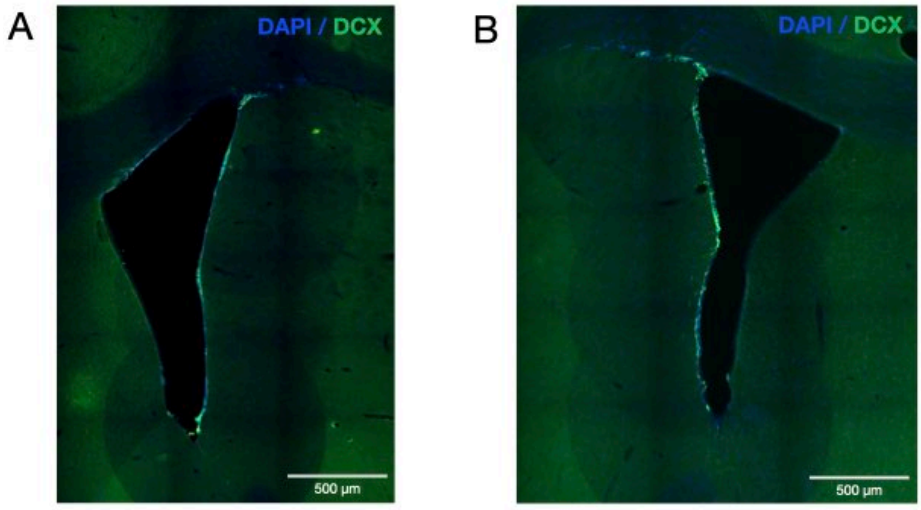

Figure 14. Representative tile scans of SVZ in C57Bl/6 mice. Staining: doublecortin (green) and nuclei (blue). (A) Vehicle treated mouse. (B) OXS-N1 treated mouse.

Discussion

In contrast to evidences from *in vitro* experiments, OXS-N1 did not show pro-neurogenic capacity *in vivo* in these experimental conditions, neither in wild type mice, nor in 5xFAD animals. We investigated its possible role in promoting the increase of immature neurones (DCX^+ cells), in stimulating proliferation of RGL cells ($GFAP^+BrdU^+$ cells), and in fostering neurogenesis ($NeuN^+BrdU^+$ cells). A potential increase in BrdU-positive cells can be interpreted also as an increase in the survival of proliferating cells, however OXS-N1 did not show an effect in this aspect neither. What we have observed instead is that OXS-N1-treated 5xFAD mice have a significantly lower density of newborn neurones in the infrapyramidal blade of GCL. The same trend in terms of newborn neurones was seen in the infrapyramidal blade of wild type mice, even if the difference between the two groups is not statistically significant. Of course this result is not what was expected and could be explained by the high intrinsic variability of the data in both vehicle and OXS-N1 treated 5xFAD mice probably given by the negative impact of the pathology on AHN (Coefficient of variation (CV) vehicle group = 0.873, CV OXS-N1 group = 0.872). However the same could be said for density calculated in the crest of the DG of 5xFAD. Indeed in both cases several mice, even analzing three 30μm sagittal brain slices for each mouse, have zero positive cells in infrapyramidal blade and crest. Instead, both groups of wild type animals show less dispersed data (CV vehicle group = 0.716, CV OXS-N1 group = 0.590). To clarify this point, it would be helpful to repeat the experiment with a higher number of mice; however, given the poor outcome also in terms of behavioural tasks, it is not worth to repeat the analysis with the same parameters.

We consider also the possibility that OXS-N1 may affect the neurogenic niche indirectly. Since neuroinflammation plays an important role in AD, we investigated the possible role of OXS-N1 in modulating this aspect of the pathology, in particular the density of microglia cells. We quantified this parameter in a subset of both 5xFAD and C57Bl/6 mice, and we did not observe changes between vehicle and OXS-N1 treated mice. A different approach could be more informative, for example the quantification of the levels of pro-inflammatory cytokines or of microglia activation. In the latter case, it would be interesting to investigate the presence of disease-associated microglial (Keren-Shaul et al., 2017) and the effect that OXS-N1 could have had on the transition from homeostatic microglia to DAM.

In order to explain the results obtained, we carefully consider the age of the mice employed in the study and the corresponding stage of the disease. At the time of treatment 5xFAD were

4.5-5.5 months old. At this time point they start to accumulate Aβ plaques in the hippocampal area, accompanied by impairment of hippocampus-dependent memory, pattern-separation included (Choi et al., 2018). At this age and stage of the pathology, some studies reported reduced DCX+ cell density in DG of 5xFAD mice compared to wild type animals (Moon et al., 2014) (Choi et al., 2018 - supplementary material), while others reported a higher density (Ziegler-Waldkirch et al., 2018). For what concerns general levels of proliferation of cells in DG, also in this case there are contrasting evidences indicating a decrease (Choi et al., 2018) or an increase (Ziegler-Waldkirch et al., 2018). Later on, when these 5xFAD animals are perfused, they are 7-8.5 months old and the disease is extremely progressed, as we qualitatively evaluated. At this time point they already show neuronal loss in pyramidal cells of layer V of the cortex and subiculum (start at 6 months of age), and the number of activated astrocytes and microglia, as well as levels of hippocampal pro-inflammatory cytokines and chemokines, are significantly increased (Oakley et al., 2006)(Choi et al., 2018). At this age, the level of DCX^+ cells has been reported to further decrease compared to younger 5xFAD animals and to age-matched WT mice (Ziegler-Waldkirch et al., 2018) (Moon et al., 2014). Additionally, considering the only other study we found in literature which reported DCX^+ cell density per volume, our value (4104 ± 2212 DCX^+ cells/mm^3) is comparable, even if higher, to the approximately 2000 cells/mm^3 that has been reported in 8-months old mice (Ziegler-Waldkirch et al., 2018). Even for the levels of proliferation in the DG at this age, it has been shown a decline compared to younger 5xFAD mice (Ziegler-Waldkirch et al., 2018).

On account of these evidences, we consider the possibility that even if OXS-N1 have had promoted an increase in the number of neuroblasts or newborn neurones in mice at 4-5 months of age, we may not see them in such old animals because of a lack of survival. To explain it more in detail, there is the possibility that new born cells at the time of drug administration, have died soon after birth because of the high levels of neuroinflammation, the accumulation of intraneuronal Aβ, the vicinity to Aβ plaques or other AD related events. In order to address this possibility, treated mice should be analyzed sooner after OXS-N1 administration, or even at different time points following the treatment, in order to assess the rate of survival. If this hypothesis was proven right, we could explain it considering that promoting AHN is not enough if at the same time a healthier brain environment that can sustain the survival of new born neurones, is not formed. This has been seen in the study of Choi et al. where neurogenesis in hippocampus of 5xFAD animals was boosted pharmacologically-genetically and when combined with an increase in BNDF levels, one of the growth factors promoted by physical exercise which is a well known AHN stimulus (van Praag et

al., 1999, van Praag et al., 2005), they increase the number of neuroblasts and at the same time they lead to an amelioration in memory tasks, mimicking exercise-induced improvements in cognition. Therefore, an interesting possibility would be to couple the administration of OXS-N1 with BNDF, or other factors that act on the neurogenic niche for example by reducing neuroinflammation, in order to increase the survival rate. As a matter of facts, activated microglia has a role in impairing hippocampal neurogenesis. One of the first studies addressing this aspect showed with an animal model of neuroinflammation, by injection of lipopolysaccharide, that an increased number of microglia cells in DG was coupled with a decreased number of DCX^+ cells. They also proved that with the administration of a common nonsteroidal anti-inflammatory drug, normal levels of neurogenesis are restored (Monje et al., 2003). Therefore, even the administration of the pro-neurogenic compound together with anti-inflammatory drugs could be a combination to unravel.

Another consideration is that there could be a specific window during the progress of the pathology in which neurogenesis can be boosted to give actual benefits, and it could be before structural changes appear in the hippocampus. In this project, OXS-N1 was administered around the are of 5 months, therefore the hippocampal region is already affected by lesions. Again, considering the study by Choi et al., they severely impaired AHN in 5xFAD mice at 6-8 weeks of age or later on at 4-5 months, and in the first case it resulted in a significant level of granule cell death once animals reach 5 months of age, while in the second it did not. Therefore, AHN impairment at a very early disease stage appears to exacerbate cell death at later stages when the DG is directly involved in the pathogenesis, hence after 4 months of age. What they concluded from these data is that adult-generated neurons at a relatively early stage of AD are critical for later maintaining the survival and stability of granule neurons. For this reason, treatment with OXS-N1 earlier in the pathology progression could result in increased AHN, protection against neuronal cell death later in the disease and actual behavioural improvement. Another evidence supporting this hypothesis is that in the same study they saw an increase in DCX^+ cells but starting the pro-neurogenic treatment in 2 months old mice.

In respect to C57Bl/6 wild type mice, we compared the density of DCX^+ cell that we calculated to values already reported in the literature. In our study, 7 month old mice present a density of 19541 ± 4521 SD /mm^3, that is, as expected, lower than the density between 23000 and 30000/mm^3 reported in 2.5 months old mice (Wang et al., 2016)(Zhang et al., 2019). The possibility to boost hippocampal neurogenesis in wild type animals has been demonstrated by several studies,

in both young and aged animals (van Praag et al., 1999, Creer et al., 2010, van Praag et al., 2005). Moreover, it has been seen that stimulation of AHN combined with voluntary exercise, produces a marked increase in behavioural tasks even is not accompanied by an increase in the number of newborn neurones compared to control mice. Therefore, the behaviour may be explained by enhanced properties of the already present excitable young newborn neurones (Sahay et al. 2011). Accordingly, another aspect to consider is that OXS-N1 could have enhanced the synaptic plasticity of already present neuroblasts and/or granule cells already mature. To address this possibility, it could be interesting to analyze the synaptic density in the ML, for example by quantifying levels of synaptic proteins by immunohistochemistry or western blot. Some markers to be used could be postsynaptic density protein 95, a constituent protein of the post-synaptic complex in excitatory synapses (Santuy et al., 2020); or synaptophysin, a pre-synaptic marker involved in synaptogenesis and which level reflects the number and density of synapses (Calhoun et al., 1996). The same could be applied in the study employing 5xFAD animals, indeed in the brain of this mouse model levels of synaptophysin decrease with age (Oakley et al., 2006), including in the DG (Kim et al., 2019).

As demonstrated by our colleges, OXS-N1 target molecule may be vimentin. As mention before, vimentin is a type III intermediate filament found in RGL cells (Seri et al., 2001). This protein has been recently proposed to have a role in maintaining cellular homeostasis by asymmetrically partitioning aggregated proteins and other damaged components in one daughter cells. This mechanism is also called replicative rejuvenation, since cells can enter mitosis in order to reverse damage accumulated during aging and increase the fitness of one of the daughter cells (Pattabiraman et al., 2020). Specifically in NSCs, vimentin has been proven to be an organizer of proteostasis-related proteins at the aggresome, a critical regulator of this program that quiescent NSCs use to clear protein through activation and mitosis. Moreover vimentin KO NSCs showed reduced proliferation, namely reduced ability to exit quiescence, and this was confirmed also *in vivo* in the SGZ of vimentin KO mice, which display also a higher age-dependent decrease in the number of neuroblasts compared to WT mice, even with equal numbers of NSCs (Morrow et al., 2020). We considered the possibility that OXS-N1 could be increasing neurogenesis by modulating quiescence in NSCs. However, we did not observe increased number of dividing NSCs ($BrdU^+GFAP^+$ cells) in both wild type and 5xFAD mice. We postulate that this could be due to the low number of NSCs in the mice used. Accordingly, as said before, future studies should aim to use less aged mice.

Conclusions

The potential therapeutic application of boosting neurogenesis to treat neurodegenerative disease is incredibly appealing. Even more considering that for Alzheimer's disease several pharmacological treatments have been approved but, for now, they show only limited efficacy.

We have seen that the progressions of AD is accompanied by neurogenesis impairments, and whether AHN impairments mediate aspects of AD pathogenesis or are a mere result of the pathological events of the disease, remains to be clarified. Indeed several studies in rodents have proven that promoting neurogenesis in normal conditions improves cognitive behaviour, and even in animal models of AD boosting AHN at certain stages of the disease has been shown to recover cognitive functions to a certain level. In this project we tested the idea of a pharmacological intervention that can promote neurogenesis and mitigate the damage of AD, using a new combination of *in vitro* screening of small molecule library and *in vivo* fully automated behavioural test battery. Several aspects of this approach can be implemented in perspective of future screenings, starting from the identification of the optimal time window to boost AHN *in vivo* which remains an unanswered and important question. Moreover, it would be worth to design experiments that allow to discriminate between the effect of increasing proliferation of NSCs and/or neuroblasts, and the effect of increasing the survival of neuroblasts and newborn neurones. In this way it would be possible to evaluate the best strategy to manipulate AHN and improve cognitive function.

An interesting finding in humans, to be confirmed by further investigations, is that individuals characterized by normal cognition, despite the presence of amyloid plaques and neurofibrillary tangles characteristic of a fully developed disease, have increased AHN compared to patients with AD-related dementia (Briley at al., 2016). Hence the idea that adult born neurones, or neuroblasts themselves with their peculiar properties, could work as neuroadaptive response to preserve cognitive functions. All things considered, boosting adult hippocampal neurogenesis or preserving the survival of neuroblasts, may result in therapeutic approaches aimed at recovering the damage of AD.

Bibliography

2022 Alzheimer's disease facts and figures. Alzheimers Dement. 2022 Apr;18(4):700-789. doi: 10.1002/alz.12638. Epub 2022 Mar 14. PMID: 35289055.

Altman J, Das GD. Autoradiographic and histological evidence of postnatal hippocampal neurogenesis in rats. J Comp Neurol. 1965 Jun;124(3):319-35. doi: 10.1002/cne.901240303. PMID: 5861717

Amaral DG, Scharfman HE, Lavenex P. The dentate gyrus: fundamental neuroanatomical organization (dentate gyrus for dummies). Prog Brain Res. 2007;163:3-22. doi: 10.1016/S0079-6123(07)63001-5. PMID: 17765709; PMCID: PMC2492885.

Andersen J, Urbán N, Achimastou A, Ito A, Simic M, Ullom K, Martynoga B, Lebel M, Göritz C, Frisén J, Nakafuku M, Guillemot F. A transcriptional mechanism integrating inputs from extracellular signals to activate hippocampal stem cells. Neuron. 2014 Sep 3;83(5):1085-97. doi: 10.1016/j.neuron.2014.08.004. PMID: 25189209; PMCID: PMC4157576.

Babcock KR, Page JS, Fallon JR, Webb AE. Adult Hippocampal Neurogenesis in Aging and Alzheimer's Disease. Stem Cell Reports. 2021 Apr 13;16(4):681-693. doi: 10.1016/j.stemcr.2021.01.019. Epub 2021 Feb 25. PMID: 33636114; PMCID: PMC8072031.

Bekris LM, Yu CE, Bird TD, Tsuang DW. Genetics of Alzheimer disease. J Geriatr Psychiatry Neurol. 2010 Dec;23(4):213-27. doi: 10.1177/0891988710383571. PMID: 21045163; PMCID: PMC3044597.

Bergmans BA, De Strooper B. gamma-secretases: from cell biology to therapeutic strategies. Lancet Neurol. 2010 Feb;9(2):215-26. doi: 10.1016/S1474-4422(09)70332-1. PMID: 20129170.

Bertrand N, Castro DS, Guillemot F. Proneural genes and the specification of neural cell types. Nat Rev Neurosci. 2002 Jul;3(7):517-30. doi: 10.1038/nrn874. PMID: 12094208.

Bischofberger J. Young and excitable: new neurons in memory networks. Nat Neurosci. 2007 Mar;10(3):273-5. doi: 10.1038/nn0307-273. PMID: 17318218.

Boldrini M, Fulmore CA, Tartt AN, Simeon LR, Pavlova I, Poposka V, Rosoklija GB, Stankov A, Arango V, Dwork AJ, Hen R, Mann JJ. Human Hippocampal Neurogenesis Persists throughout Aging. Cell Stem Cell. 2018 Apr 5;22(4):589-599.e5. doi: 10.1016/j.stem.2018.03.015. PMID: 29625071; PMCID: PMC5957089.

Bonaguidi MA, Wheeler MA, Shapiro JS, Stadel RP, Sun GJ, Ming GL, Song H. In vivo clonal analysis reveals self-renewing and multipotent adult neural stem cell characteristics. Cell. 2011 Jun 24;145(7):1142-55. doi: 10.1016/j.cell.2011.05.024. Epub 2011 Jun 16. PMID: 21664664; PMCID: PMC3124562

Braak H, Braak E. Neuropathological stageing of Alzheimer-related changes. Acta Neuropathol. 1991;82(4):239-59. doi: 10.1007/BF00308809. PMID: 1759558.

Braak H, Braak E. Staging of Alzheimer's disease-related neurofibrillary changes. Neurobiol Aging. 1995 May-Jun;16(3):271-8; discussion 278-84. doi: 10.1016/0197-4580(95)00021-6. PMID: 7566337.

Braak H, Braak E. Neuropil threads occur in dendrites of tangle-bearing nerve cells. Neuropathol Appl Neurobiol. 1988 Jan-Feb;14(1):39-44. doi: 10.1111/j.1365-2990.1988.tb00864.x. PMID: 2453810.

Brandt MD, Jessberger S, Steiner B, Kronenberg G, Reuter K, Bick-Sander A, von der Behrens W, Kempermann G. Transient calretinin expression defines early postmitotic step of neuronal differentiation in adult hippocampal neurogenesis of mice. Mol Cell Neurosci. 2003 Nov;24(3):603-13. doi: 10.1016/s1044-7431(03)00207-0. PMID: 14664811.

Briley D, Ghirardi V, Woltjer R, Renck A, Zolochevska O, Taglialatela G, Micci MA. Preserved neurogenesis in non-demented individuals with AD neuropathology. Sci Rep. 2016 Jun 14;6:27812. doi: 10.1038/srep27812. PMID: 27298190; PMCID: PMC4906289.

Brown JP, Couillard-Després S, Cooper-Kuhn CM, Winkler J, Aigner L, Kuhn HG. Transient expression of doublecortin during adult neurogenesis. J Comp Neurol. 2003 Dec 1;467(1):1-10. doi: 10.1002/cne.10874. PMID: 14574675.

Brunden KR, Trojanowski JQ, Lee VM. Advances in tau-focused drug discovery for Alzheimer's disease and related tauopathies. Nat Rev Drug Discov. 2009 Oct;8(10):783-93. doi: 10.1038/nrd2959. PMID: 19794442; PMCID: PMC2787232

Bu G. Apolipoprotein E and its receptors in Alzheimer's disease: pathways, pathogenesis and therapy. Nat Rev Neurosci. 2009 May;10(5):333-44. doi: 10.1038/nrn2620. Epub 2009 Apr 2. PMID: 19339974; PMCID: PMC2908393.

Carlesimo GA, Piras F, Orfei MD, Iorio M, Caltagirone C, Spalletta G. Atrophy of presubiculum and subiculum is the earliest hippocampal anatomical marker of Alzheimer's disease. Alzheimers Dement (Amst). 2015 Mar 29;1(1):24-32. doi: 10.1016/j.dadm.2014.12.001. PMID: 27239489; PMCID: PMC4876901.

Calhoun ME, Jucker M, Martin LJ, Thinakaran G, Price DL, Mouton PR. Comparative evaluation of synaptophysin-based methods for quantification of synapses. J Neurocytol. 1996 Dec;25(12):821-8. doi: 10.1007/BF02284844. PMID: 9023727.

Chauhan P, Jethwa K, Rathawa A, Chauhan G, Mehra S. The Anatomy of the Hippocampus. In: Pluta R, editor. Cerebral Ischemia [Internet]. Brisbane (AU): Exon Publications; 2021 Nov 6. Chapter 2. PMID: 34905307.

Chen GF, Xu TH, Yan Y, Zhou YR, Jiang Y, Melcher K, Xu HE. Amyloid beta: structure, biology and structure-based therapeutic development. Acta Pharmacol Sin. 2017 Sep;38(9):1205-1235. doi: 10.1038/aps.2017.28. Epub 2017 Jul 17. PMID: 28713158; PMCID: PMC5589967

Chen M, Puschmann TB, Marasek P, Inagaki M, Pekna M, Wilhelmsson U, Pekny M. Increased Neuronal Differentiation of Neural Progenitor Cells Derived from Phosphovimentin-Deficient Mice. Mol Neurobiol. 2018 Jul;55(7):5478-5489. doi: 10.1007/s12035-017-0759-0. Epub 2017 Sep 27. PMID: 28956310; PMCID: PMC5994207.

Cheng XR, Zhou WX, Zhang YX. The behavioral, pathological and therapeutic features of the senescence-accelerated mouse prone 8 strain as an Alzheimer's disease animal model. Ageing Res Rev. 2014 Jan; 13:13-37. doi: 10.1016/j.arr.2013.10.002. Epub 2013 Nov 21. PMID: 24269312.

Choi SH, Bylykbashi E, Chatila ZK, Lee SW, Pulli B, Clemenson GD, Kim E, Rompala A, Oram MK, Asselin C, Aronson J, Zhang C, Miller SJ, Lesinski A, Chen JW, Kim DY, van Praag H, Spiegelman BM, Gage FH, Tanzi RE. Combined adult neurogenesis and BDNF mimic exercise effects on cognition in an Alzheimer's mouse model. Science. 2018 Sep 7;361(6406):eaan8821. doi: 10.1126/science.aan8821. PMID: 30190379; PMCID: PMC6149542.

Clelland CD, Choi M, Romberg C, Clemenson GD Jr, Fragniere A, Tyers P, Jessberger S, Saksida LM, Barker RA, Gage FH, Bussey TJ. A functional role for adult hippocampal neurogenesis in spatial pattern separation. Science. 2009 Jul 10;325(5937):210-3. doi: 10.1126/science.1173215. PMID: 19590004; PMCID: PMC2997634.

Corder EH, Saunders AM, Strittmatter WJ, Schmechel DE, Gaskell PC, Small GW, Roses AD, Haines JL, Pericak-Vance MA. Gene dose of apolipoprotein E type 4 allele and the risk of Alzheimer's disease in late onset families. Science. 1993 Aug 13;261(5123):921-3. doi: 10.1126/science.8346443. PMID: 8346443.

Creer DJ, Romberg C, Saksida LM, van Praag H, Bussey TJ. Running enhances spatial pattern separation in mice. Proc Natl Acad Sci U S A. 2010 Feb 2;107(5):2367-72. doi: 10.1073/pnas.0911725107. Epub 2010 Jan 19. PMID: 20133882; PMCID: PMC2836679.

Cunningham CL, Martínez-Cerdeño V, Noctor SC. Microglia regulate the number of neural precursor cells in the developing cerebral cortex. J Neurosci. 2013 Mar 6;33(10):4216-33. doi: 10.1523/JNEUROSCI. 3441-12.2013. PMID: 23467340; PMCID: PMC3711552.

Curtis MA, Kam M, Faull RL. Neurogenesis in humans. Eur J Neurosci. 2011 Mar;33(6):1170-4. doi: 10.1111/j.1460-9568.2011.07616.x. PMID: 21395861.

DeTure MA, Dickson DW. The neuropathological diagnosis of Alzheimer's disease. Mol Neurodegener. 2019 Aug 2;14(1):32. doi: 10.1186/s13024-019-0333-5. PMID: 31375134; PMCID: PMC6679484.

Deng W, Aimone JB, Gage FH. New neurons and new memories: how does adult hippocampal neurogenesis affect learning and memory? Nat Rev Neurosci. 2010 May;11(5):339-50. doi: 10.1038/nrn2822. Epub 2010 Mar 31. PMID: 20354534; PMCID: PMC2886712.

Dennis CV, Suh LS, Rodriguez ML, Kril JJ, Sutherland GT. Human adult neurogenesis across the ages: An immunohistochemical study. Neuropathol Appl Neurobiol. 2016 Dec;42(7):621-638. doi: 10.1111/nan.12337. Epub 2016 Aug 28. PMID: 27424496; PMCID: PMC5125837.

Doetsch F, Alvarez-Buylla A. Network of tangential pathways for neuronal migration in adult mammalian brain. Proc Natl Acad Sci U S A. 1996 Dec 10;93(25):14895-900. doi: 10.1073/pnas.93.25.14895. PMID: 8962152; PMCID: PMC26233.

Doetsch F. A niche for adult neural stem cells. Curr Opin Genet Dev. 2003 Oct;13(5):543-50. doi: 10.1016/j.gde.2003.08.012. PMID: 14550422.

Encinas JM, Michurina TV, Peunova N, Park JH, Tordo J, Peterson DA, Fishell G, Koulakov A, Enikolopov G. Division-coupled astrocytic differentiation and age-related depletion of neural stem cells in the adult hippocampus. Cell Stem Cell. 2011 May 6;8(5):566-79. doi: 10.1016/j.stem.2011.03.010. PMID: 21549330; PMCID: PMC3286186.

Eriksson PS, Perfilieva E, Björk-Eriksson T, Alborn AM, Nordborg C, Peterson DA, Gage FH. Neurogenesis in the adult human hippocampus. Nat Med. 1998 Nov;4(11):1313-7. doi: 10.1038/3305. PMID: 9809557.

Erwin SR, Sun W, Copeland M, Lindo S, Spruston N, Cembrowski MS. A Sparse, Spatially Biased Subtype of Mature Granule Cell Dominates Recruitment in Hippocampal-Associated Behaviors. Cell Rep. 2020 Apr 28;31(4):107551. doi: 10.1016/j.celrep.2020.107551. PMID: 32348756.

Fanselow MS, Dong HW. Are the dorsal and ventral hippocampus functionally distinct structures? Neuron. 2010 Jan 14;65(1):7-19. doi: 10.1016/j.neuron.2009.11.031. PMID: 20152109; PMCID: PMC2822727.

Filippov V, Kronenberg G, Pivneva T, Reuter K, Steiner B, Wang LP, Yamaguchi M, Kettenmann H, Kempermann G. Subpopulation of nestin-expressing progenitor cells in the adult murine hippocampus shows electrophysiological and morphological characteristics of astrocytes. Mol Cell Neurosci. 2003 Jul;23(3):373-82. doi: 10.1016/s1044-7431(03)00060-5. PMID: 12837622.

Flor-García M, Terreros-Roncal J, Moreno-Jiménez EP, Ávila J, Rábano A, Llorens-Martín M. Unraveling human adult hippocampal neurogenesis. Nat Protoc. 2020 Feb;15(2):668-693. doi: 10.1038/s41596-019-0267-y. Epub 2020 Jan 8. PMID: 31915385.

Fu H, Hardy J, Duff KE. Selective vulnerability in neurodegenerative diseases. Nat Neurosci. 2018 Oct;21(10):1350-1358. doi: 10.1038/s41593-018-0221-2. Epub 2018 Sep 24. PMID: 30250262; PMCID: PMC6360529.

Fukuda S, Kato F, Tozuka Y, Yamaguchi M, Miyamoto Y, Hisatsune T. Two distinct subpopulations of nestin-positive cells in adult mouse dentate gyrus. J Neurosci. 2003 Oct 15;23(28):9357-66. doi: 10.1523/JNEUROSCI.23-28-09357.2003. Erratum in: J Neurosci. 2004 Jan 7;24(1):24. PMID: 14561863; PMCID: PMC6740569.

Gage FH, Coates PW, Palmer TD, Kuhn HG, Fisher LJ, Suhonen JO, Peterson DA, Suhr ST, Ray J. Survival and differentiation of adult neuronal progenitor cells transplanted to the adult brain. Proc Natl Acad Sci U S A. 1995 Dec 5;92(25):11879-83. doi: 10.1073/pnas.92.25.11879. PMID: 8524867; PMCID: PMC40506.

Garcia AD, Doan NB, Imura T, Bush TG, Sofroniew MV. GFAP-expressing progenitors are the principal source of constitutive neurogenesis in adult mouse forebrain. Nat Neurosci. 2004 Nov;7(11):1233-41. doi: 10.1038/nn1340. Epub 2004 Oct 24. PMID: 15494728.

Gault N, Szele FG. Immunohistochemical evidence for adult human neurogenesis in health and disease. WIREs Mech Dis. 2021 Nov;13(6):e1526. doi: 10.1002/wsbm.1526. Epub 2021 Apr 1. PMID: 34730290.

Gheusi G, Cremer H, McLean H, Chazal G, Vincent JD, Lledo PM. Importance of newly generated neurons in the adult olfactory bulb for odor discrimination. Proc Natl Acad Sci U S A. 2000 Feb 15;97(4):1823-8. doi: 10.1073/pnas.97.4.1823. PMID: 10677540; PMCID: PMC26520.

a) Gould E, Reeves AJ, Fallah M, Tanapat P, Gross CG, Fuchs E. Hippocampal neurogenesis in adult Old World primates. Proc Natl Acad Sci U S A. 1999 Apr 27;96(9):5263-7. doi: 10.1073/pnas.96.9.5263. PMID: 10220454; PMCID: PMC21852

b) Gould E, Beylin A, Tanapat P, Reeves A, Shors TJ. Learning enhances adult neurogenesis in the hippocampal formation. Nat Neurosci. 1999 Mar;2(3):260-5. doi: 10.1038/6365. PMID: 10195219.

Greenwood EK, Angelova DM, Büchner HMI, Brown DR. The AICD fragment of APP initiates a FoxO3a mediated response via FANCD2. Mol Cell Neurosci. 2022 Sep;122:103760. doi: 10.1016/j.mcn.2022.103760. Epub 2022 Jul 25. PMID: 35901928

Heneka MT, Carson MJ, El Khoury J, Landreth GE, Brosseron F, Feinstein DL, Jacobs AH, Wyss-Coray T, Vitorica J, Ransohoff RM, Herrup K, Frautschy SA, Finsen B, Brown GC, Verkhratsky A, Yamanaka K, Koistinaho J, Latz E, Halle A, Petzold GC, Town T, Morgan D, Shinohara ML, Perry VH, Holmes C, Bazan NG, Brooks DJ, Hunot S, Joseph B, Deigendesch N, Garaschuk O, Boddeke E, Dinarello CA, Breitner JC, Cole GM, Golenbock DT, Kummer MP. Neuroinflammation in Alzheimer's disease. Lancet Neurol. 2015 Apr;14(4):388-405. doi: 10.1016/S1474-4422(15)70016-5. PMID: 25792098; PMCID: PMC5909703.

Hoogmartens J, Cacace R, Van Broeckhoven C. Insight into the genetic etiology of Alzheimer's disease: A comprehensive review of the role of rare variants. Alzheimers Dement (Amst). 2021 Feb 20;13(1):e12155. doi: 10.1002/dad2.12155. PMID: 33665345; PMCID: PMC7896636.

Hopperton KE, Mohammad D, Trépanier MO, Giuliano V, Bazinet RP. Markers of microglia in post-mortem brain samples from patients with Alzheimer's disease: a systematic review. Mol Psychiatry. 2018 Feb;23(2):177-198. doi: 10.1038/mp.2017.246. Epub 2017 Dec 12. PMID: 29230021; PMCID: PMC5794890

Iwano T, Masuda A, Kiyonari H, Enomoto H, Matsuzaki F. Prox1 postmitotically defines dentate gyrus cells by specifying granule cell identity over CA3 pyramidal cell fate in the hippocampus. Development. 2012 Aug;139(16):3051-62. doi: 10.1242/dev.080002. Epub 2012 Jul 12. PMID: 22791897.

Jensen JB, Parmar M. Strengths and limitations of the neurosphere culture system. Mol Neurobiol. 2006 Dec;34(3):153-61. doi: 10.1385/MN:34:3:153. PMID: 17308349.

Jin K, Peel AL, Mao XO, Xie L, Cottrell BA, Henshall DC, Greenberg DA. Increased hippocampal neurogenesis in Alzheimer's disease. Proc Natl Acad Sci U S A. 2004 Jan 6;101(1):343-7. doi: 10.1073/pnas.2634794100. Epub 2003 Dec 5. PMID: 14660786; PMCID: PMC314187.

Kempermann G, Kuhn HG, Gage FH. Genetic influence on neurogenesis in the dentate gyrus of adult mice. Proc Natl Acad Sci U S A. 1997 Sep 16;94(19):10409-14. doi: 10.1073/pnas.94.19.10409. PMID: 9294224; PMCID: PMC23376.

Kempermann G, Kuhn HG, Gage FH. Experience-induced neurogenesis in the senescent dentate gyrus. J Neurosci. 1998 May 1;18(9):3206-12. doi: 10.1523/JNEUROSCI.18-09-03206.1998. PMID: 9547229; PMCID: PMC6792643.

Kempermann G, Gast D, Kronenberg G, Yamaguchi M, Gage FH. Early determination and long-term persistence of adult-generated new neurons in the hippocampus of mice. Development. 2003 Jan;130(2): 391-9. doi: 10.1242/dev.00203. PMID: 12466205.

Kempermann G, Jessberger S, Steiner B, Kronenberg G. Milestones of neuronal development in the adult hippocampus. Trends Neurosci. 2004 Aug;27(8):447-52. doi: 10.1016/j.tins.2004.05.013. PMID: 15271491.

Keren-Shaul H, Spinrad A, Weiner A, Matcovitch-Natan O, Dvir-Szternfeld R, Ulland TK, David E, Baruch K, Lara-Astaiso D, Toth B, Itzkovitz S, Colonna M, Schwartz M, Amit I. A Unique Microglia Type Associated with Restricting Development of Alzheimer's Disease. Cell. 2017 Jun 15;169(7):1276-1290.e17. doi: 10.1016/j.cell.2017.05.018. Epub 2017 Jun 8. PMID: 28602351.

Kim S, Nam Y, Jeong YO, Park HH, Lee SK, Shin SJ, Jung H, Kim BH, Hong SB, Park YH, Kim J, Yu J, Yoo DH, Park SH, Jeon SG, Moon M. Topographical Visualization of the Reciprocal Projection between the Medial Septum and the Hippocampus in the 5XFAD Mouse Model of Alzheimer's Disease. Int J Mol Sci. 2019 Aug 16;20(16):3992. doi: 10.3390/ijms20163992. PMID: 31426329; PMCID: PMC6721212.

Knoth R, Singec I, Ditter M, Pantazis G, Capetian P, Meyer RP, Horvat V, Volk B, Kempermann G. Murine features of neurogenesis in the human hippocampus across the lifespan from 0 to 100 years. PLoS One. 2010 Jan 29;5(1):e8809. doi: 10.1371/journal.pone.0008809. PMID: 20126454; PMCID: PMC2813284

Kornack DR, Rakic P. Continuation of neurogenesis in the hippocampus of the adult macaque monkey. Proc Natl Acad Sci U S A. 1999 May 11;96(10):5768-73. doi: 10.1073/pnas.96.10.5768. PMID: 10318959; PMCID: PMC21935.

Kriegstein A, Alvarez-Buylla A. The glial nature of embryonic and adult neural stem cells. Annu Rev Neurosci. 2009;32:149-84. doi: 10.1146/annurev.neuro.051508.135600. PMID: 19555289; PMCID: PMC3086722.

Kuhn HG, Dickinson-Anson H, Gage FH. Neurogenesis in the dentate gyrus of the adult rat: age-related decrease of neuronal progenitor proliferation. J Neurosci. 1996 Mar 15;16(6):2027-33. doi: 10.1523/JNEUROSCI.16-06-02027.1996. PMID: 8604047; PMCID: PMC6578509

Lazarov O, Mattson MP, Peterson DA, Pimplikar SW, van Praag H. When neurogenesis encounters aging and disease. Trends Neurosci. 2010 Dec;33(12):569-79. doi: 10.1016/j.tins.2010.09.003. Epub 2010 Oct 18. PMID: 20961627; PMCID: PMC2981641.

Lendahl U, Zimmerman LB, McKay RD. CNS stem cells express a new class of intermediate filament protein. Cell. 1990 Feb 23;60(4):585-95. doi: 10.1016/0092-8674(90)90662-x. PMID: 1689217.

Leng F, Edison P. Neuroinflammation and microglial activation in Alzheimer disease: where do we go from here? Nat Rev Neurol. 2021 Mar;17(3):157-172. doi: 10.1038/s41582-020-00435-y. Epub 2020 Dec 14. PMID: 33318676.

Leung KK, Bartlett JW, Barnes J, Manning EN, Ourselin S, Fox NC; Alzheimer's Disease Neuroimaging Initiative. Cerebral atrophy in mild cognitive impairment and Alzheimer disease: rates and acceleration. Neurology. 2013 Feb 12;80(7):648-54. doi: 10.1212/WNL.0b013e318281ccd3. Epub 2013 Jan 9. PMID: 23303849; PMCID: PMC3590059.

Li Puma DD, Piacentini R, Grassi C. Does Impairment of Adult Neurogenesis Contribute to Pathophysiology of Alzheimer's Disease? A Still Open Question. Front Mol Neurosci. 2021 Jan 22;13:578211. doi: 10.3389/fnmol.2020.578211. PMID: 33551741; PMCID: PMC7862134

Lim DA, Alvarez-Buylla A. The Adult Ventricular-Subventricular Zone (V-SVZ) and Olfactory Bulb (OB) Neurogenesis. Cold Spring Harb Perspect Biol. 2016 May 2;8(5):a018820. doi: 10.1101/cshperspect.a018820. PMID: 27048191; PMCID: PMC4852803.

Liu CC, Liu CC, Kanekiyo T, Xu H, Bu G. Apolipoprotein E and Alzheimer disease: risk, mechanisms and therapy. Nat Rev Neurol. 2013 Feb;9(2):106-18. doi: 10.1038/nrneurol.2012.263. Epub 2013 Jan 8. Erratum in: Nat Rev Neurol. 2013. doi: 10.1038/nmeurol.2013.32. Liu, Chia-Chan [corrected to Liu, Chia-Chen]. PMID: 23296339; PMCID: PMC3726719.

Lois C, Alvarez-Buylla A. Proliferating subventricular zone cells in the adult mammalian forebrain can differentiate into neurons and glia. Proc Natl Acad Sci U S A. 1993 Mar 1;90(5):2074-7. doi: 10.1073/pnas.90.5.2074. PMID: 8446631; PMCID: PMC46023

Maekawa M, Takashima N, Arai Y, Nomura T, Inokuchi K, Yuasa S, Osumi N. Pax6 is required for production and maintenance of progenitor cells in postnatal hippocampal neurogenesis. Genes Cells. 2005 Oct;10(10):1001-14. doi: 10.1111/j.1365-2443.2005.00893.x. PMID: 16164600.

Moon M, Cha MY, Mook-Jung I. Impaired hippocampal neurogenesis and its enhancement with ghrelin in 5XFAD mice. J Alzheimers Dis. 2014;41(1):233-41. doi: 10.3233/ JAD-132417. PMID: 24583405.

Monje ML, Toda H, Palmer TD. Inflammatory blockade restores adult hippocampal neurogenesis. Science. 2003 Dec 5;302(5651):1760-5. doi: 10.1126/science.1088417. Epub 2003 Nov 13. PMID: 14615545.

Morrow CS, Porter TJ, Xu N, Arndt ZP, Ako-Asare K, Heo HJ, Thompson EAN, Moore DL. Vimentin Coordinates Protein Turnover at the Aggresome during Neural Stem Cell Quiescence Exit. Cell Stem Cell. 2020 Apr 2;26(4):558-568.e9. doi: 10.1016/j.stem.2020.01.018. Epub 2020 Feb 27. PMID: 32109376; PMCID: PMC7127969.

Mucke L, Masliah E, Yu GQ, Mallory M, Rockenstein EM, Tatsuno G, Hu K, Kholodenko D, Johnson-Wood K, McConlogue L. High-level neuronal expression of abeta 1-42 in wild-type human amyloid protein precursor transgenic mice: synaptotoxicity without plaque formation. J Neurosci. 2000 Jun 1;20(11):4050-8. doi: 10.1523/JNEUROSCI.20-11-04050.2000. PMID: 10818140; PMCID: PMC6772621.

Mullen RJ, Buck CR, Smith AM. NeuN, a neuronal specific nuclear protein in vertebrates. Development. 1992 Sep;116(1):201-11. doi: 10.1242/dev.116.1.201. PMID: 1483388.

Nazarian A, Yashin AI, Kulminski AM. Genome-wide analysis of genetic predisposition to Alzheimer's disease and related sex disparities. Alzheimers Res Ther. 2019 Jan 12;11(1):5. doi: 10.1186/s13195-018-0458-8. PMID: 30636644; PMCID: PMC6330399.

Neurobiology of Brain Disorders - Biological Basis of Neurological and Psychiatric Disorders, 1st Edition, November 25, 2014,

Zigmond M, Coyle J, Rowland L. Neurobiology of Brain Disorders - Biological Basis of Neurological and Psychiatric Disorders. 1st ed. Academic Press; November 25, 2014.

O'Brien RJ, Wong PC. Amyloid precursor protein processing and Alzheimer's disease. Annu Rev Neurosci. 2011;34:185-204. doi: 10.1146/annurev-neuro-061010-113613. PMID: 21456963; PMCID: PMC3174086

Oakley H, Cole SL, Logan S, Maus E, Shao P, Craft J, Guillozet-Bongaarts A, Ohno M, Disterhoft J, Van Eldik L, Berry R, Vassar R. Intraneuronal beta-amyloid aggregates, neurodegeneration, and neuron loss in transgenic mice with five familial Alzheimer's disease mutations: potential factors in amyloid plaque formation. J Neurosci. 2006 Oct 4;26(40):10129-40. doi: 10.1523/JNEUROSCI. 1202-06.2006. PMID: 17021169; PMCID: PMC6674618.

Oblak AL, Lin PB, Kotredes KP, Pandey RS, Garceau D, Williams HM, Uyar A, O'Rourke R, O'Rourke S, Ingraham C, Bednarczyk D, Belanger M, Cope ZA, Little GJ, Williams SG, Ash C, Bleckert A, Ragan T, Logsdon BA, Mangravite LM, Sukoff Rizzo SJ, Territo PR, Carter GW, Howell GR, Sasner M, Lamb BT. Comprehensive Evaluation of the 5XFAD Mouse Model for Preclinical Testing Applications: A MODEL-AD Study. Front Aging Neurosci. 2021 Jul 23;13:713726. doi: 10.3389/fnagi.2021.713726. PMID: 34366832; PMCID: PMC8346252.

Palmer TD, Takahashi J, Gage FH. The adult rat hippocampus contains primordial neural stem cells. Mol Cell Neurosci. 1997;8(6):389-404. doi: 10.1006/mcne.1996.0595. PMID: 9143557.

Pattabiraman S, Azad GK, Amen T, Brielle S, Park JE, Sze SK, Meshorer E, Kaganovich D. Vimentin protects differentiating stem cells from stress. Sci Rep. 2020 Nov 11;10(1):19525. doi: 10.1038/s41598-020-76076-4. PMID: 33177544; PMCID: PMC7658978.

Peeters G, Katelekha K, Lawlor B, Demnitz N. Sex differences in the incidence and prevalence of young-onset Alzheimer's disease: A meta-analysis. Int J Geriatr Psychiatry. 2021 Aug 12;37(1):10.1002/gps.5612. doi: 10.1002/gps.5612. Epub ahead of print. PMID: 34386999; PMCID: PMC9290036.

Penke Z, Chagneau C, Laroche S. Contribution of Egr1/zif268 to Activity-Dependent Arc/Arg3.1 Transcription in the Dentate Gyrus and Area CA1 of the Hippocampus. Front Behav Neurosci. 2011 Aug 17;5:48. doi: 10.3389/fnbeh.2011.00048. PMID: 21887136; PMCID: PMC3156974.

Reynolds BA, Weiss S. Generation of neurons and astrocytes from isolated cells of the adult mammalian central nervous system. Science. 1992 Mar 27;255(5052):1707-10. doi: 10.1126/science.1553558. PMID: 1553558.

Reynolds BA, Weiss S. Clonal and population analyses demonstrate that an EGF-responsive mammalian embryonic CNS precursor is a stem cell. Dev Biol. 1996 Apr 10;175(1):1-13. doi: 10.1006/dbio.1996.0090. PMID: 8608856.

Richter SH. Automated Home-Cage Testing as a Tool to Improve Reproducibility of Behavioral Research? Front Neurosci. 2020 Apr 24;14:383. doi: 10.3389/fnins.2020.00383. PMID: 32390795; PMCID: PMC7193758.

Sahay A, Scobie KN, Hill AS, O'Carroll CM, Kheirbek MA, Burghardt NS, Fenton AA, Dranovsky A, Hen R. Increasing adult hippocampal neurogenesis is sufficient to improve pattern separation. Nature. 2011 Apr 28;472(7344):466-70. doi: 10.1038/nature09817. Epub 2011 Apr 3. PMID: 21460835; PMCID: PMC3084370.

Sala-Jarque J, Zimkowska K, Ávila J, Ferrer I, Del Río JA. Towards a Mechanistic Model of Tau-Mediated Pathology in Tauopathies: What Can We Learn from Cell-Based In Vitro Assays? Int J Mol Sci. 2022 Sep 29;23(19):11527. doi: 10.3390/ijms231911527. PMID: 36232835; PMCID: PMC9570106.

Sanchez-Varo R, Mejias-Ortega M, Fernandez-Valenzuela JJ, Nuñez-Diaz C, Caceres-Palomo L, Vegas-Gomez L, Sanchez-Mejias E, Trujillo-Estrada L, Garcia-Leon JA, Moreno-Gonzalez I, Vizuete M, Vitorica J, Baglietto-Vargas D, Gutierrez A. Transgenic Mouse Models of Alzheimer's Disease: An Integrative Analysis. Int J Mol Sci. 2022 May 12;23(10):5404. doi: 10.3390/ijms23105404. PMID: 35628216; PMCID: PMC9142061.

Santuy A, Tomás-Roca L, Rodríguez JR, González-Soriano J, Zhu F, Qiu Z, Grant SGN, DeFelipe J, Merchan-Perez A. Estimation of the number of synapses in the hippocampus and brain-wide by volume electron microscopy and genetic labeling. Sci Rep. 2020 Aug 19;10(1):14014. doi: 10.1038/s41598-020-70859-5. PMID: 32814795; PMCID: PMC7438319.

Sasmono RT, Oceandy D, Pollard JW, Tong W, Pavli P, Wainwright BJ, Ostrowski MC, Himes SR, Hume DA. A macrophage colony-stimulating factor receptor-green fluorescent protein transgene is expressed throughout the mononuclear phagocyte system of the mouse. Blood. 2003 Feb 1;101(3):1155- 63. doi: 10.1182/blood-2002-02-0569. Epub 2002 Sep 12. PMID: 12393599.

Schmechel DE, Saunders AM, Strittmatter WJ, Crain BJ, Hulette CM, Joo SH, Pericak-Vance MA, Goldgaber D, Roses AD. Increased amyloid beta-peptide deposition in cerebral cortex as a consequence of apolipoprotein E genotype in late-onset Alzheimer disease. Proc Natl Acad Sci U S A. 1993 Oct 15;90(20): 9649-53. doi: 10.1073/pnas.90.20.9649. PMID: 8415756; PMCID: PMC47627.

Schmidt-Hieber C, Jonas P, Bischofberger J. Enhanced synaptic plasticity in newly generated granule cells of the adult hippocampus. Nature. 2004 May 13;429(6988):184-7. doi: 10.1038/nature02553. Epub 2004 Apr 25. PMID: 15107864.

Seki T, Arai Y. Highly polysialylated neural cell adhesion molecule (NCAM-H) is expressed by newly generated granule cells in the dentate gyrus of the adult rat. J Neurosci. 1993 Jun;13(6):2351-8. doi: 10.1523/JNEUROSCI.13-06-02351.1993. PMID: 7684771; PMCID: PMC6576495

Seri B, García-Verdugo JM, McEwen BS, Alvarez-Buylla A. Astrocytes give rise to new neurons in the adult mammalian hippocampus. J Neurosci. 2001 Sep 15;21(18):7153-60. doi: 10.1523/JNEUROSCI.21-18-07153.2001. PMID: 11549726; PMCID: PMC6762987.

Seri B, García-Verdugo JM, Collado-Morente L, McEwen BS, Alvarez-Buylla A. Cell types, lineage, and architecture of the germinal zone in the adult dentate gyrus. J Comp Neurol. 2004 Oct 25;478(4):359-78. doi: 10.1002/cne.20288. Erratum in: J Comp Neurol. 2004 Dec 20;480(4):427. PMID: 15384070.

Shin J, Park S, Lee H, Kim Y. Thioflavin-positive tau aggregates complicating quantification of amyloid plaques in the brain of 5XFAD transgenic mouse model. Sci Rep. 2021 Jan 15;11(1):1617. doi: 10.1038/s41598-021-81304-6. PMID: 33452414; PMCID: PMC7810901.

Siegel G, Gerber H, Koch P, Bruestle O, Fraering PC, Rajendran L. The Alzheimer's Disease γ-Secretase Generates Higher 42:40 Ratios for β-Amyloid Than for p3 Peptides. Cell Rep. 2017 Jun 6;19(10):1967-1976. doi: 10.1016/j.celrep.2017.05.034. PMID: 28591569.

Sierra A, Encinas JM, Deudero JJ, Chancey JH, Enikolopov G, Overstreet-Wadiche LS, Tsirka SE, Maletic-Savatic M. Microglia shape adult hippocampal neurogenesis through apoptosis-coupled phagocytosis. Cell Stem Cell. 2010 Oct 8;7(4):483-95. doi: 10.1016/j.stem.2010.08.014. PMID: 20887954; PMCID: PMC4008496.

Snyder HM, Asthana S, Bain L, Brinton R, Craft S, Dubal DB, Espeland MA, Gatz M, Mielke MM, Raber J, Rapp PR, Yaffe K, Carrillo MC. Sex biology contributions to vulnerability to Alzheimer's disease: A think tank convened by the Women's Alzheimer's Research Initiative. Alzheimers Dement. 2016 Nov;12(11): 1186-1196. doi: 10.1016/j.jalz.2016.08.004. Epub 2016 Sep 27. PMID: 27692800.

Soares R, Ribeiro FF, Lourenço DM, Rodrigues RS, Moreira JB, Sebastião AM, Morais VA, Xapelli S. Isolation and Expansion of Neurospheres from Postnatal (P1-3) Mouse Neurogenic Niches. J Vis Exp. 2020 May 23;(159). doi: 10.3791/60822. PMID: 32510488.

Sorrells SF, Paredes MF, Cebrian-Silla A, Sandoval K, Qi D, Kelley KW, James D, Mayer S, Chang J, Auguste KI, Chang EF, Gutierrez AJ, Kriegstein AR, Mathern GW, Oldham MC, Huang EJ, Garcia-Verdugo JM, Yang Z, Alvarez-Buylla A. Human hippocampal neurogenesis drops sharply in children to undetectable levels in adults. Nature. 2018 Mar 15;555(7696):377-381. doi: 10.1038/nature25975. Epub 2018 Mar 7. PMID: 29513649; PMCID: PMC6179355.

Spalding KL, Bergmann O, Alkass K, Bernard S, Salehpour M, Huttner HB, Boström E, Westerlund I, Vial C, Buchholz BA, Possnert G, Mash DC, Druid H, Frisén J. Dynamics of hippocampal neurogenesis in adult humans. Cell. 2013 Jun 6;153(6):1219-1227. doi: 10.1016/j.cell.2013.05.002. PMID: 23746839; PMCID: PMC4394608.

Steiner B, Kronenberg G, Jessberger S, Brandt MD, Reuter K, Kempermann G. Differential regulation of gliogenesis in the context of adult hippocampal neurogenesis in mice. Glia. 2004 Apr 1;46(1):41-52. doi: 10.1002/glia.10337. PMID: 14999812.

Suh H, Consiglio A, Ray J, Sawai T, D'Amour KA, Gage FH. In vivo fate analysis reveals the multipotent and self-renewal capacities of Sox2+ neural stem cells in the adult hippocampus. Cell Stem Cell. 2007 Nov; 1(5):515-28. doi: 10.1016/j.stem.2007.09.002. PMID: 18371391; PMCID: PMC2185820.

Terreros-Roncal J, Moreno-Jiménez EP, Flor-García M, Rodríguez-Moreno CB, Trinchero MF, Cafini F, Rábano A, Llorens-Martín M. Impact of neurodegenerative diseases on human adult hippocampal neurogenesis. Science. 2021 Nov 26;374(6571):1106-1113. doi: 10.1126/science.abl5163. Epub 2021 Oct 21. PMID: 34672693; PMCID: PMC7613437.

Hsia AY, Masliah E, McConlogue L, Yu GQ, Tatsuno G, Hu K, Kholodenko D, Malenka RC, Nicoll RA, Mucke L. Plaque-independent disruption of neural circuits in Alzheimer's disease mouse models. Proc Natl Acad Sci U S A. 1999 Mar 16;96(6):3228-33. doi: 10.1073/pnas.96.6.3228. PMID: 10077666; PMCID: PMC15924.

Urbán N, van den Berg DL, Forget A, Andersen J, Demmers JA, Hunt C, Ayrault O, Guillemot F. Return to quiescence of mouse neural stem cells by degradation of a proactivation protein. Science. 2016 Jul 15;353(6296):292-5. doi: 10.1126/science.aaf4802. PMID: 27418510; PMCID: PMC5321528.

van Praag H, Kempermann G, Gage FH. Running increases cell proliferation and neurogenesis in the adult mouse dentate gyrus. Nat Neurosci. 1999 Mar;2(3):266-70. doi: 10.1038/6368. PMID: 10195220.

van Praag H, Schinder AF, Christie BR, Toni N, Palmer TD, Gage FH. Functional neurogenesis in the adult hippocampus. Nature. 2002 Feb 28;415(6875):1030-4. doi: 10.1038/4151030a. PMID: 11875571; PMCID: PMC9284568.

Wang X, Gao X, Michalski S, Zhao S, Chen J. Traumatic Brain Injury Severity Affects Neurogenesis in Adult Mouse Hippocampus. J Neurotrauma. 2016 Apr 15;33(8):721-33. doi: 10.1089/neu.2015.4097. Epub 2015 Dec 2. PMID: 26414411; PMCID: PMC4841001.

Wightman DP, Jansen IE, Savage JE, Shadrin AA, Bahrami S, Holland D, Rongve A, Børte S, Winsvold BS, Drange OK, Martinsen AE, Skogholt AH, Willer C, Bråthen G, Bosnes I, Nielsen JB, Fritsche LG, Thomas LF, Pedersen LM, Gabrielsen ME, Johnsen MB, Meisingset TW, Zhou W, Proitsi P, Hodges A, Dobson R, Velayudhan L, Heilbron K, Auton A; 23andMe Research Team, Sealock JM, Davis LK, Pedersen NL, Reynolds CA, Karlsson IK, Magnusson S, Stefansson H, Thordardottir S, Jonsson PV, Snaedal J, Zettergren A, Skoog I, Kern S, Waern M, Zetterberg H, Blennow K, Stordal E, Hveem K, Zwart JA, Athanasiu L, Selnes P, Saltvedt I, Sando SB, Ulstein I, Djurovic S, Fladby T, Aarsland D, Selbæk G, Ripke S, Stefansson K, Andreassen OA, Posthuma D. A genome-wide association study with 1,126,563 individuals identifies new risk loci for Alzheimer's disease. Nat Genet. 2021 Sep;53(9):1276-1282. doi: 10.1038/s41588-021-00921-z. Epub 2021 Sep 7. Erratum in: Nat Genet. 2021 Dec;53(12):1722. Erratum in: Nat Genet. 2022 Jul;54(7): 1062. PMID: 34493870.

Winner B, Winkler J. Adult neurogenesis in neurodegenerative diseases. Cold Spring Harb Perspect Biol. 2015 Apr 1;7(4):a021287. doi: 10.1101/cshperspect.a021287. PMID: 25833845; PMCID: PMC4382734.

Zaletel I, Schwirtlich M, Perović M, Jovanović M, Stevanović M, Kanazir S, Puškaš N. Early Impairments of Hippocampal Neurogenesis in 5xFAD Mouse Model of Alzheimer's Disease Are Associated with Altered Expression of SOXB Transcription Factors. J Alzheimers Dis. 2018;65(3): 963-976. doi: 10.3233/ JAD-180277. PMID: 30103323

Zhao C, Teng EM, Summers RG Jr, Ming GL, Gage FH. Distinct morphological stages of dentate granule neuron maturation in the adult mouse hippocampus. J Neurosci. 2006 Jan 4;26(1):3-11. doi: 10.1523/ JNEUROSCI.3648-05.2006. PMID: 16399667; PMCID: PMC6674324.

Zhou Y, Su Y, Li S, Kennedy BC, Zhang DY, Bond AM, Sun Y, Jacob F, Lu L, Hu P, Viaene AN, Helbig I, Kessler SK, Lucas T, Salinas RD, Gu X, Chen HI, Wu H, Kleinman JE, Hyde TM, Nauen DW, Weinberger DR, Ming GL, Song H. Molecular landscapes of human hippocampal immature neurons across lifespan. Nature. 2022 Jul;607(7919):527-533. doi: 10.1038/s41586-022-04912-w. Epub 2022 Jul 6. PMID: 35794479; PMCID: PMC9316413.

Ziebell F, Dehler S, Martin-Villalba A, Marciniak-Czochra A. Revealing age-related changes of adult hippocampal neurogenesis using mathematical models. Development. 2018 Jan 8;145(1):dev153544. doi: 10.1242/dev.153544. PMID: 29229768; PMCID: PMC5825879.

Ziegler-Waldkirch S, d'Errico P, Sauer JF, Erny D, Savanthrapadian S, Loreth D, Katzmarski N, Blank T, Bartos M, Prinz M, Meyer-Luehmann M. Seed-induced Aβ deposition is modulated by microglia under environmental enrichment in a mouse model of Alzheimer's disease. EMBO J. 2018 Jan 17;37(2):167-182. doi: 10.15252/embj.201797021. Epub 2017 Dec 11. PMID: 29229786; PMCID: PMC5770788.